

# NAVAL POSTGRADUATE SCHOOL Monterey, California



## THESIS

COMPARISON OF ALKALI ION EMITTERS

by

Dean Alan Gant

December 1991

Thesis Advisor:

R.C. Olsen

Approved for public release; distribution is unlimited.



REPORT DOCUMENTATION PAGE				Form Approved OMB No. 0704-0188	
1a. REPORT SECURITY CLASSIFICATION <b>UNCLASSIFIED</b>			1b. RESTRICTIVE MARKINGS		
2a. SECURITY CLASSIFICATION AUTHORITY			3. DISTRIBUTION / AVAILABILITY OF REPORT Approved for public release; distribution is unlimited.		
2b. DECLASSIFICATION / DOWNGRADING SCHEDULE			4. PERFORMING ORGANIZATION REPORT NUMBER(S)		
4. PERFORMING ORGANIZATION REPORT NUMBER(S)			5. MONITORING ORGANIZATION REPORT NUMBER(S)		
6a. NAME OF PERFORMING ORGANIZATION <b>Naval Postgraduate School</b>		6b. OFFICE SYMBOL (If applicable) <b>33</b>	7a. NAME OF MONITORING ORGANIZATION <b>Naval Postgraduate School</b>		
6c. ADDRESS (City, State, and ZIP Code) <b>Monterey, CA 93943-5000</b>			7b. ADDRESS (City, State, and ZIP Code) <b>Monterey, CA 93943-5000</b>		
8a. NAME OF FUNDING / SPONSORING ORGANIZATION		8b. OFFICE SYMBOL (If applicable)	9. PROCUREMENT INSTRUMENT IDENTIFICATION NUMBER		
8c. ADDRESS (City, State, and ZIP Code)			10. SOURCE OF FUNDING NUMBERS		
			PROGRAM ELEMENT NO.	PROJECT NO.	TASK NO.
			WORK UNIT ACCESSION NO.		
11. TITLE (Include Security Classification) <b>COMPARISON OF ALKALI ION EMITTERS</b>					
12. PERSONAL AUTHOR(S) <b>Dean Alan Gant</b>					
13a. TYPE OF REPORT <b>Master's Thesis</b>		13b. TIME COVERED FROM _____ TO _____	14. DATE OF REPORT (Year, Month, Day) <b>December 1991</b>		15. PAGE COUNT <b>93</b>
16. SUPPLEMENTARY NOTATION <b>The views expressed in this thesis are those of the author and do not reflect the official policy or position of the Department of Defense or the U.S. Government.</b>					
17. COSATI CODES			18. SUBJECT TERMS (Continue on reverse if necessary and identify by block number)		
FIELD	GROUP	SUB-GROUP	alkali ion emitters		
19. ABSTRACT (Continue on reverse if necessary and identify by block number) Lithium, Potassium, and Cesium ion sources have been studied using devices based on thermal emission from a Beta-Eucryptite structure as possible ion sources for use in satellite charge control. The experiments evaluated the power requirements of the different ion emitters to produce approximately 10(microamps) of current and tested the effects of using an Osmium-Ruthenium coating to increase the work function of the emitter surface. Lifetime tests of the different ion emitters were also performed. Analysis of the experimental findings showed that Lithium ion sources with a lifetime of 93 hours and Potassium ion sources with a lifetime of 44 hours produced acceptable current levels for use in spacecraft charge control devices. Potassium sources produced the necessary current, 10(microamps), at 140°(C) lower temperature than the Lithium sources. All of the coated sources produced wildly fluctuating currents at the 10(microamp) level and were not acceptable for the purpose intended.					
20. DISTRIBUTION / AVAILABILITY OF ABSTRACT <input checked="" type="checkbox"/> UNCLASSIFIED/UNLIMITED <input type="checkbox"/> SAME AS RPT. <input type="checkbox"/> DTIC USERS			21. ABSTRACT SECURITY CLASSIFICATION <b>Unclassified</b>		
22a. NAME OF RESPONSIBLE INDIVIDUAL <b>R. C. Olsen</b>			22b. TELEPHONE (Include Area Code) <b>(408)646-2019</b>		22c. OFFICE SYMBOL <b>PH/0s</b>

Approved for public release; distribution is unlimited.

COMPARISON OF ALKALI ION EMITTERS

by

Dean Alan Gant  
Captain, United States Army  
B.S., United States Military Academy, 1983

Submitted in partial fulfillment of the  
requirements for the degree of

MASTER OF SCIENCE IN PHYSICS

from the

NAVAL POSTGRADUATE SCHOOL  
December 1991

Author:



Dean Alan Gant

Approved By:



R. C. Olsen, Thesis Advisor



O. Heinz, Second Reader



K. E. Woehler, Chairman,  
Department of Physics

## ABSTRACT

Lithium, Potassium, and Cesium ion sources have been studied using devices based on thermal emission from a Beta-Eucryptite structure as possible ion sources for use in satellite charge control. The experiments evaluated the power requirements of the different ion emitters to produce approximately  $10(\mu\text{A})$  of current and tested the effects of using an Osmium-Ruthenium coating to increase the work function of the emitter surface. Lifetime tests of the different ion emitters were also performed. Analysis of the experimental findings showed that Lithium ion sources with a lifetime of 93 hours and Potassium ion sources with a lifetime of 44 hours produced acceptable current levels for use in spacecraft charge control devices. Potassium sources produced the necessary current,  $10(\mu\text{A})$ , at  $140^{\circ}\text{C}$  lower temperature than the Lithium sources. All of the coated sources produced wildly fluctuating currents at the  $10(\mu\text{A})$  level and were not acceptable for the purpose intended.

# TABLE OF CONTENTS

I.	INTRODUCTION.....	1
II.	BACKGROUND.....	3
	A. SPACECRAFT CHARGING.....	3
	B. SPACECRAFT CHARGE CONTROL.....	6
III.	THEORY.....	10
	A. ION EMISSION.....	10
	B. BETA-EUCRYPTITE.....	10
IV.	ION SOURCES.....	13
	A. INTRODUCTION.....	13
	B. ION SOURCE STRUCTURE.....	13
	C. EMITTING COMPOUNDS.....	14
V.	EXPERIMENTAL EQUIPMENT.....	16
	A. VACUUM SYSTEM.....	16
	B. VACUUM CHAMBER.....	16
	C. ION GUN.....	17

VI.	EXPERIMENTAL OBSERVATIONS.....	19
A.	LITHIUM ION SOURCES.....	19
B.	POTASSIUM ION SOURCES.....	23
C.	POTASSIUM ION SOURCES WITH COATING.....	26
D.	CESIUM ION SOURCE.....	30
E.	CESIUM ION SOURCES WITH COATING.....	33
VII.	SOURCE COMPARISON.....	36
A.	SOURCE LIFETIMES.....	36
B.	POWER AND TEMPERATURE.....	37
C.	EXTRACTION POTENTIAL.....	39
VIII.	CONCLUSIONS.....	41
	APPENDIX.....	42
	LIST OF REFERENCES.....	82
	INITIAL DISTRIBUTION LIST.....	85



# I. INTRODUCTION

Satellite charge control technology is needed to improve satellite survivability at high altitudes and to improve the results of scientific measurements on research missions. Plasma (ion) sources are needed to reduce the positive charge induced on illuminated surfaces, by photoemission, and to reduce differential, negative, charge buildup on shadowed insulators. Previous experimental work on satellite charge control devices at the Naval Postgraduate School considered gas discharge technology (hollow cathodes) and, more recently, solid state ion emitters.[Ref.1,2] The solid state devices considered to date utilized Lithium ion production. These emitters produced sufficient ions, approximately  $10(\mu\text{A})$ , for use in charge control devices. One drawback of the lithium sources was that the power requirements were greater than the desired power of approximately  $15(\text{W})$ . This thesis pursues the use of ion emitters which produced Potassium or Cesium ions instead of Lithium ions. The idea is to determine if the power requirements for ion emitters could be reduced by using other alkali elements with lower ionization energies than Lithium without decreasing the source lifetimes or current production below the levels required. Increased ion source

lifetime and lower power requirements would increase the usefulness of the sources as charge control devices on space vehicles.

The work described below is based on the operation of an ion emitter design which uses a tungsten pellet impregnated with different emitter materials which have a common, Beta-Eucryptite, crystalline structure. Lithium, Potassium, and Cesium ion emitters were tested. The experiments were designed to evaluate the power requirements to produce approximately  $10(\mu\text{A})$  of current, the level which would be necessary for the ion source to be used as part of a space vehicle charge control device. Tests were done on the effects of coating the surface of the emitter with an Osmium-Ruthenium layer to increase the work function of the emitter surface. The lifetimes of ion sources with different emitter materials were also tested.

## II. BACKGROUND

### A. SPACECRAFT CHARGING

#### 1. History

Spacecraft charging is defined as the potential difference between the surface of a spacecraft and the surrounding plasma. Such potentials result from the interaction of space vehicles with sunlight and the surrounding plasma. In sunlight, high altitude satellites typically float a few volts positive.[Ref.3] In the absence of sunlight, potentials comparable to the energy of the ambient electrons can develop. Negative potentials on spacecraft ranging from 0(V) to -10,000(V) in eclipse were first reported by DeForest in 1972 when observed by detectors on ATS-5 (Applied Technology Satellite-5). DeForest also reported that typical satellite potentials at geosynchronous orbit in sunlight range from -200(V) to a few volts positive. Further measurements of negative potentials were observed by detectors on ATS-6 (Applied Technology Satellite-6) and SCATHA (Spacecraft Charging at High Altitude) satellites. Olsen reported the largest observed negative potential to date, -19,000(V) in eclipse and -2,000(V) in sunlight, which occurred on ATS-6.[Refs.4,5,6,7]

The occurrence of negative satellite potentials in sunlight was something of a mystery, since the current due to photoemission was so much larger than the ambient plasma (electron) current. The resolution of the mystery involves the process of differential charging which is the development of large negative potentials on shadowed surfaces.[Ref.8]

## 2. Charging Effects

Spacecraft charging, defined as the buildup of charge on the satellite frame, may blind some environmental sensors but is not a major problem by itself. Charging becomes a problem, endangering satellites and their operation, when a potential difference develops between adjacent surfaces. This potential difference can lead to arcing. Arcing, which is nature's way of balancing the charges, is observed and reported as spacecraft operational anomalies. Arcing can be a serious problem and it is possible for satellites to be structurally damaged by strong discharges. In addition, weak discharges have been related to unusual electronic switching incidents, thermal coating breakdown, and degradation of solar cell and optical sensor operations. The initial correspondence between spacecraft charging and operational anomalies came from comparing the time distribution of the potentials measured on ATS-6, shown in Figure 1(a), with the time distribution of operational

anomalies shown in Figure 1(b). This comparison showed that spacecraft anomalies occur more frequently during periods of increased potential as measured by detectors on the satellite. The detailed analysis of a major charging event on the SCATHA satellite, in September 1982, established a clear link between satellite charging, arcing, and operational anomalies on the SCATHA satellite.[Refs.4,9,10,11]

### 3. Charging Sources

#### *a, Photoelectric Effect*

Typically, the largest current at geosynchronous orbit is produced by the Photoelectric effect. Photons which collide with the surface of the spacecraft can knock electrons from the spacecraft's surface. As electrons leave the surface through photoemission the surface builds up a positive charge as shown in Figure 2.[Ref.3,12]

#### *b, Space Plasma*

The ambient space plasma also contributes to surface charging. A spacecraft is constantly colliding with charged particles, which are collected on the surface of the satellite. Surfaces in shadow will typically build up a net negative charge as shown in Figure 2. This is because the flux ( $nv_{th}$ ) of the electrons is approximately 43 times the ambient ion flux for a Hydrogen ion environment. Some

spacecraft geometries can actually enhance this effect by having depressions in the surface of the spacecraft.[Refs.4,9,13]

*c, Differential Charging*

The spacecraft would charge to a uniform potential if the materials making up the surface were uniform good conductors. Satellite surface materials, however, are selected mainly for their thermal properties which leads to the majority of the spacecraft's surface being made of insulators instead of conductors. Also, solar arrays are made up of glass covered cells. Therefore, there is a wide difference in the conductivity between different areas of the surface. This conductivity difference leads to differential charging in which the sunlit areas of the satellite can charge positively, while the shaded areas develop a negative charge.[Ref.4,12,13]

## B. SPACECRAFT CHARGE CONTROL

### 1. Passive Control

The photoelectric effect and plasma bombardment combine to generate the majority of spacecraft surface charging. Many aspects of vehicle design including stabilization techniques, material makeup, and orbital positioning may vary the generation of surface charge due to these processes. In particular, spacecraft design using

conducting materials for surface construction and proper grounding can eliminate a large percentage of charging problems. Also, the photoelectric effect and plasma bombardment do offset each other to a certain extent as would be expected. However, realistic design restrictions and some specific satellite missions eliminate the possibility of sufficient charge control through manufacturing techniques and orbital placement.[Ref.4,9]

## 2. Active Control

Active control of spacecraft charging would require a satellite to be equipped with ion and electron emitters capable of producing sufficient quantities of charged particles that when emitted from the satellite would neutralize the effects of charging on the frame and insulating surfaces. For science missions, typically utilizing conductive coatings over the insulators, an ion emitter would be necessary to neutralize the positive spacecraft potentials encountered in sunlight to allow measurements of the very cold component of the ambient plasma.[Ref.14,15]

## 3. Observation of Charge Control

The effects of plasma emissions on spacecraft potentials were reported by Olsen in 1981. Observations of the charging effects on ATS-6 in conjunction with the operation of an ion engine were examined to determine the

effect of plasma emission on satellite surface charging. Data analysis showed that plasma emission could be used to control spacecraft charging and differential surface charging.[Ref.16]

Ion engine technology, as applied to charge control, utilizes a gas discharge. The core of this technology is the hollow cathode. Such a device is scheduled to fly in 1993 on the National Aeronautic and Space Administration Polar satellite. The technology has some drawbacks. The gas feed system, including pressure vessel, valve, and regulator is heavy. The system can be difficult to integrate and electromagnetically noisy. Weight and power limitations led to a new charge control design for use on the Cluster satellite. This design is a 7(kV), 10( $\mu$ A), liquid metal, Indium ion gun. The limitation of this design is that it does not affect differential charging, since the 7(kV) ion beam does not return to the vehicle.[Ref.15]

#### 4. Charge Control Device

Concerns about the problems associated with gas discharge technology motivated a search for a different design. This search led to studies using the Lithium ion source developed by Heinz and Reaves [Ref.22]. This source has been previously studied at the Naval Postgraduate School [Ref.2]. One implementation of this design using the same principles as the previous work at the Naval Postgraduate

School is shown in Figure 3. This device, invented by P. L. Leung, is a quiet plasma source which produces a plasma from separate ion and electron emitters. Leung's plasma source is designed for use in examining space plasma effects and can be used as a charge neutralizer without causing the electromagnetic interference associated with producing ions using impact ionization discharges in neutral gases. This thesis will investigate the types of ion sources, which could be used in a source like this one for spacecraft charge control.[Ref.17]

### III. THEORY

#### A. ION EMISSION

Ions are easily produced by placing certain materials on the surface of a heated metal filament. The coating of impurities can be evaporated as positive ions as long as the work function of the surface of the filament exceeds the ionization potential of the atom that is evaporating. This principle is used extensively in mass spectrograph studies such as research for unknown stable isotopes.[Ref.18,19]

Blewett and Jones compared several alkali aluminosilicate sources using this process by heating coated tungsten spiral filaments. Of the aluminosilicates tested, Beta-eucryptite was the most satisfactory producer of ions. It produced almost twice the current at a given temperature as the next best source. At 170(°C) below its melting point it produced as much as 1 (mA) of current.[Ref.20]

#### B. BETA-EUCRYPTITE

##### 1. Structure

Beta-Eucryptite ( $\text{Li}_2\text{O}-\text{Al}_2\text{O}_3-2\text{SiO}_2$ ) is an aluminosilicate with a crystalline structure as shown in Figure 4. Its structure is similar to high temperature

quartz with the exception that half of the Silicon atoms are replaced by Aluminum atoms in alternate layers along the c axis. The Lithium atoms are situated in large holes in the center of the lattice structure and bound to Oxygen atoms. These Oxygen atoms also have electrostatic bonds to one Silicon and one Aluminum atom. The bonds to the Silicon and Aluminum atoms are much stronger than the bonds to the Lithium atom. When heated this difference in bond strength causes the structure to expand in such a way that the centrally located openings in the lattice are increased in diameter. The Lithium molecules, located in these opening are then easily released when an electric field is applied.[Ref.21]

## 2. Production Mechanism

Crystal conglomerates of Beta-Eucryptite, which were essentially single crystals, have been examined in order to determine the conducting mechanism within the lattice structure. Measurements of the thermoelectric power of Beta-Eucryptite showed that the crystal was p-type. This is consistent with having a concentration gradient of positively charged Lithium atoms oriented along the thickness of the crystal. This explanation was confirmed by observing that Lithium ion production is increased when the emitting plane is perpendicular to the symmetry axis.[Ref.21]

### 3. Conclusion

Therefore, the structural analysis and experimental results indicate that Lithium ions travel through channels in the crystal structure which are enhanced by heating the crystal. This makes the structure of Beta-Eucryptite an excellent configuration for the production of ions.

## IV. ION SOURCES

### A. INTRODUCTION

The ion sources used in the experimental work of this thesis were produced by Spectra-Mat Incorporated of Watsonville, California. These sources are based on a design by O. Heinz and R. T. Reaves. The source takes advantage of the nonuniform crystalline expansion of Beta-Eucryptite in conjunction with the high work function of a porous tungsten disc. The source, coated with Beta-Eucryptite, when heated is a copious ion producer. It is used in conjunction with an extraction grid, placed at a negative potential, which overcomes the ion vapor pressure at the emitting surface and accelerates the ions away from the source.[Ref.21]

### B. ION SOURCE STRUCTURE

Based on the fact that crystalline compounds of Beta-Eucryptite would emit Lithium ions when heated above 1000(°C), Heinz and Reaves designed a compact Lithium emitter in 1968 which is shown in Figure 5. This source was described as follows.

The emitter consists of an indirectly heated, highly porous, tungsten plug into which the emitter material has been fused. The molybdenum body holding the tungsten plug is machined with a solid partition for complete isolation between the emitter and the heater cavity. The three rhenium support struts are brazed at a 120° spacing with a moly/ruthenium eutectic at 2100°C in hydrogen, yielding a ductile and versatile mounting tripod. The heater is a noninductively wound bifilar coil with heliarc welded rhenium leads solidly potted into the body cavity. The high purity Al<sub>2</sub>O<sub>3</sub> potting mix is H<sub>2</sub> fired at 1900(°C) which completely immobilizes the heater. The emitter matrix, a specially prepared, extremely porous, tungsten disc with a density of 30% (70% porosity) is heliarc welded to the moly body.[Ref.22]

## C. EMITTING COMPOUNDS

### 1. Compound Composition

The ion sources examined in this thesis were coated with Beta-Eucryptite compounds. They were prepared by placing an ion emitter impregnate mixture of 1 mole of alkali or alkaline earth carbonate, 2 moles of silica and 1 mole of alumina on the surface of the porous tungsten disc and melting the mixture onto the disc at approximately 1650(°C) in a Hydrogen atmosphere. The alkali or alkaline earth carbonates are greater than 99.5% pure. The silica is 140 mesh powder and the alumina is 0.05 micron alumina.[Ref.22,23]

### 2. Impregnate Mixtures

Three different impregnate mixtures were examined in this thesis. All three were prepared as described with different alkali elements. These elements were Lithium,

Potassium, and Cesium. It is assumed that the Potassium and Cesium atoms replace the Lithium atoms in the structure of Beta-Eucryptite without changing the crystalline structure of the lattice. In addition, some Potassium and Lithium sources were coated with a 1 Angstrom coating of Osmium-Ruthenium to reduce the work function of the surface.

### 3. Production Differences

During conversations with Spectra-Mat representatives, some differences in the actual production of emitters with these different impregnates were discussed. When the Lithium mixture is melted on the surface of the disc, heating is reduced as soon as the mixture glasses over. As the device cools, a portion of the impregnate pops off the surface. This leaves a deposit of Lithium impregnate on the surface which is flat and requires no further processing. When Potassium and Cesium are used, the same process is followed but all of the impregnate remains on the surface of the disc. This leaves an unacceptable surface which is flattened by grinding a portion of the impregnate off of the surface. This suggests that the actual amount of impregnate deposited on the surface is not as controllable when Lithium impregnate is used. In addition, none of the impregnate mixtures can be completely melted into the tungsten plug without evaporating the alkali atoms in the process.

## V. EXPERIMENTAL EQUIPMENT

The experimental equipment consisted of a vacuum system used to produce a high vacuum in a chamber, various potential and current measuring equipment, and a power supply to provide power to the emitting source heater. The emitting source was mounted in a specially designed ion gun.

### A. VACUUM SYSTEM

A Varian vacuum system was used to provide an experimental environment of  $10^{-3}$  to  $10^{-7}$ (torr). The Varian system used is equipped with a turbo-pump to produce high vacuum pumping. The normal operation pressure for experiments was  $1.3 \times 10^{-7}$ (torr). This system is not equipped with a liquid nitrogen trap.

### B. VACUUM CHAMBER

The vacuum chamber was a large glass bell jar. All electrical connections were made through standard vacuum connectors on the bottom plate of the chamber. A copper mesh screen was wrapped around the entire interior of the chamber and used to collect ions which traveled through the extraction grid.

## C. ION GUN

The ion gun, shown in Figure 6, was centrally mounted in the bell jar. It was designed to electrically isolate the extraction grid from the emitter source and the source mounting plate. The electrical circuit used during the experiments is shown in Figure 7. Ceramic tubing, cut to the proper length, was used to isolate the connecting bolts and also used as spacers to separate the plates of the ion gun. The spacers allowed the experiments to be standardized with the extraction grid positioned .25(in) from the surface of the emitter source.

### 1. Extraction Grid

The extraction grid was constructed from a thin sheet of tantalum. A 1/32(in) drill bit was used to perforate a circular area 1 inch in diameter in the center of the 3.5(in) diameter circular sheet. The exact transparency of the grid was not directly measured. The holes are spaced as closely as the machining process would allow causing the grid to be approximately 40% transparent.

### 2. Mounting Plate

The emitter source is mounted on a thin tantalum sheet which is attached to the center of a 1/4(in) thick aluminum disc for stability. The tantalum sheet has a central hole allowing the heater leads to pass through the

mounting plate. There are also small holes placed to line up with the support struts attached to the emitter source. During mounting the struts are easily bent over on the back of the mounting sheet to keep the emitter in position.

### 3. Support Plate

All electrical connections are made on the back of the support plate. The support plate also has a central hole to allow the connections to the emitter's heater to pass through the support plate.

## VI. EXPERIMENTAL OBSERVATIONS

All of the emitter sources were mounted in the same ion gun and positioned .25 inches from the extraction grid. Ion production was measured as a current flowing to the extraction grid and the copper screen surrounding the inside of the vacuum chamber. The total current produced by a source is reported as the sum of these two currents. The temperature of the source was measured with an optical pyrometer focusing on the side of the canister in which the source was contained. Frontal temperature measurements of the actual emitting surface were not possible because the transparency of the extraction grid was not sufficient to allow accurate readings through the grid. During normal operations the screen potential was maintained at -200(V) and the extraction grid potential was maintained at -100(V).

### A. LITHIUM ION SOURCES

Two Lithium sources were tested during these experiments. The first source was used to exhaustion for the purpose of lifetime testing. The second source was used to verify that the results of the first source were reproducible.

## 1. Lifetime

The first Lithium ion source was slowly heated until it reached  $1100(^{\circ}\text{C})$ . This temperature was maintained over a period of days. The source was operated approximately 8 hours a day and power was turned completely off each night. The vacuum ( $10^{-7}$  torr) was maintained at all times. Figure 8 shows the operating lifetime of the source. The lithium source current production increased each time it was operated through approximately 90 hours as shown in the figure. It reached a peak of  $30(\mu\text{A})$  before ion production began falling rapidly. Figure 9 is an expanded graph of the final hours of current production for the Lithium source. The decrease in current is attributed to the depletion of Lithium within the source. After 93 hours and 32 minutes the source was producing less than  $2(\mu\text{A})$  of current and was removed from the ion gun.

## 2. Power and Temperature

The power to the heater was incrementally decreased once the source was steadily producing ions to examine the current production as a function of power and as a function of the temperature corresponding to that power. Figure 10 shows that ion production for the Lithium source does not reach  $1(\mu\text{A})$  until the source reaches a temperature of  $945(^{\circ}\text{C})$  at a power of  $17(\text{W})$ . The current increased steadily as the heater power was increased. At temperatures over

1150(°C) the heater showed signs of gradual failure as power had to be gradually increased to maintain a constant temperature.

### 3. Extraction Potential

Figure 11 shows the total current as a function of extraction grid potential. The grid potential was decreased from -100(V) to -10(V) while maintaining a constant temperature. The screen potential was also held constant while the grid sweep was performed. The figure shows that ion production is increased with an increase in extraction potential. The current production does not appear to flatten out before reaching -100(V) extraction potential. Figure 11 also shows the breakdown between the current collected on the grid and the screen. The grid current is always higher and both currents increase at the same rate with an increase in extraction voltage.

### 4. Screen Potential

Figure 12 shows that varying the screen potential from -100(V) to -300(V) has no effect on the production of ions. This demonstrates that the negative potential on the collecting screen is not influencing the electric field involved in the production of the Lithium ions. Also, space charge effects outside the source region can be ignored.

## 5. Lithium Source Comparison

### *a, Power*

Figure 13 shows the total current production of the two Lithium sources as a function of applied heater power. The first source produced approximately the same number of ions at almost 6(W) less power. One of the sources could have been in better thermal contact with the mounting plate which could account for a portion of this power difference. Also, there could have been manufacturing differences, such as in heater placement, which could account for the difference in power requirements between the sources. No experiments were performed to determine the relationship between these two possible causes for different heater power requirements. Figure 13 also shows that the two Lithium sources perform much the same when ion production is compared as a function of temperature. However, the first source does produce slightly more current at all temperature settings.

### *b, Temperature and Grid Potential*

Figure 14 shows the effect of varying the grid potential at various temperatures. It shows that although more ions are produced at higher temperatures the difference in production is not realized until the grid potential is -50(V) or higher.

## B. POTASSIUM ION SOURCES

Three Potassium ion sources were used in these experiments. The first and second sources were run to exhaustion for the purpose of lifetime testing and verification of ion production. The third source failed after 1 hour of operation. The third source was operating at 895(°C) and 15.7(W) when an unexplained arc between the source and the extraction grid was observed. The arc current was sufficient to blow the fuse in the multimeter measuring current to the extraction grid. The vacuum pressure remained at  $2.2 \times 10^{-7}$ (torr) before and after this event. It is possible that a large quantity of Potassium ionized at the same time causing this arc. After this event the source was exhausted. No ion production occurred regardless of increased temperature or extraction potential.

### 1. Lifetime

The Potassium sources were slowly heated to 930(°C). Several grid and power sweeps were performed and then the sources were operated at 885(°C) for a period of days. Power was increased and reduced daily as described for previous sources. The lifetime current production of the first source is shown in Figure 15. Current production fell below 2( $\mu$ A) after 16 hours of operation. The extraction potential was increased to -200(V) in an attempt to extend

the life of the source. Current production promptly increased to  $6(\mu\text{A})$ . After an additional 18 hours the current again fell below  $2(\mu\text{A})$  and the extraction potential was increased to  $-300(\text{V})$ . The increase to  $-300(\text{V})$  increased the current production to  $4(\mu\text{A})$  but the current gradually decreased to below  $2(\mu\text{A})$  within 5 hours and the source was removed from the ion gun.

## 2. Power and Temperature

The heater power was slowly decreased after the source had been operated for several hours. Current production as a function of power and temperature for the first Potassium source is shown in Figure 16. Current production increased with increasing power. This source produced  $1(\mu\text{A})$  of current at  $790(^{\circ}\text{C})$  and  $9(\text{W})$  power.

## 3. Extraction Potential

Figure 17 shows the total current as a function of extraction grid potential for the first Potassium ion source. The grid potential was increase to  $-200(\text{V})$  and then decreased to  $-10(\text{V})$  while maintaining a constant temperature and a constant screen potential. This figure shows that Potassium ion production is also increased with increased extraction potential with the sharpest increase occurring from  $-10(\text{V})$  to  $-70(\text{V})$ . Figure 17 also shows that the grid

current is always greater than the screen current and both currents increase at the same rate with increased extraction potential.

#### 4. Potassium Source Comparison

##### *a, Lifetime*

Figure 18 shows the data from Figure 15 with the data from a second Potassium source added. Both sources produced currents above  $2(\mu\text{A})$  for approximately 16 hours with an extraction potential of  $-100(\text{V})$ . The second source was initially operated at a higher temperature and produced more current during that time which would account for the difference in lifetime between the two sources. Both sources immediately increase current production to  $7(\mu\text{A})$  when the extraction potential was increased to  $-200(\text{V})$ . The  $-200(\text{V})$  extraction potential caused both sources to produce currents above  $2(\mu\text{A})$  for an additional 20 hours. The grid potential was then raised to  $-300(\text{V})$  which increased the life of each source an additional 5 hours.

##### *b, Power*

Figure 19 shows total current production of the two Potassium sources as a function of applied heater power and the corresponding temperature. The figure shows that the two sources performed relatively the same although the first source produced higher currents for similar temperatures. This difference is probably due to initially

operating the second source at higher temperatures causing a large initial depletion of the second Potassium source. Comparison of the power and temperature curves does show that the heater in the first source is performing more efficiently. This is probably due to manufacturing differences, since operating techniques were fairly standard by this point.

### *c, Temperature and Grid Potential*

Figure 20 shows the effect of varying the grid potential at various temperatures. It shows that for the second Potassium source an increase in temperature causes an increase in ion production at all extraction potentials. However, the first source produced more ions than the second source at all temperatures and their ion production is essentially equal with a temperature difference of 40(°C). This difference is again due to the second source being operated at higher temperatures early in the experiment and being more depleted of Potassium than the first source when the measurements in Figure 20 were made.

## C. POTASSIUM ION SOURCES WITH COATING

Two Potassium ion sources with Osmium-Ruthenium coating were tested. The first source was used to exhaustion for the purpose of lifetime testing. The second source was used to verify the results from the first source.

## 1. Lifetime

The first coated Potassium source was slowly heated to 930(°C) and several experiments varying the potential and heater power were then performed. Figure 21 shows the operating lifetime of the source. After 9 hours of operation an arc was observed between the extraction grid and the source while operating at 910(°C) and 16.64(W) of power. The extraction grid potential was set at -200(V). After the arc, the current dropped from 43.67(μA) to 10(μA) and then climbed to 32(μA) in a matter of minutes. The vacuum pressure remained at  $2.0 \times 10^{-7}$ (torr) during this event. The arc is unexplained but it is possible that a large quantity of Potassium ionized at the same time causing the arc. Throughout the life of this source the current production was very unstable. At times, the current would vary as much as 10(μA) in a matter of seconds. This fluctuation was probably due to the presence of the Osmium-Ruthenium coating. The coating increases the work function of the surface. This apparently causes inconsistent ion production in the current production range over which these sources were operating. The source was then run to exhaustion with a grid potential of -200(V) and a screen potential of -100(V). These settings reduced the current fluctuation as much as possible.

## 2. Power and Temperature

The power to the heater was varied once the source had run for several hours. Figure 22 shows the ion production for both coated Potassium sources as a function of power and temperature. These sources produce  $1(\mu\text{A})$  of current at  $7(\text{W})$  to  $9(\text{W})$  of power and a temperature of  $760(^{\circ}\text{C})$ . Ion production increases with temperature until approximately  $860(^{\circ}\text{C})$  where the curve flattens out. The data points for total current are averages of the current as it varied sharply over short time intervals. For example, a reading varying from  $5(\mu\text{A})$  to  $15(\mu\text{A})$  was reported as  $10(\mu\text{A})$ . Current production was therefore much more unstable than the figure indicates.

## 3. Extraction Potential

Figure 23 shows the total current as a function of extraction grid potential for the first coated Potassium source. The grid potential was lowered from  $-200(\text{V})$  to  $-10(\text{V})$  while maintaining a constant temperature and screen potential. This figure shows that Potassium ion production is also increased with increased extraction potential with the sharpest increase occurring from  $-10(\text{V})$  to  $-90(\text{V})$ . Figure 23 also shows that the grid current is always greater than the screen current and both currents increase at the

same rate with increased extraction potential. Again, current production was more unstable than the figure indicates.

#### 4. Coated Potassium Source Comparison

##### *a, Power*

Figure 22 shows the total current production of the two coated Potassium sources as a function of applied heater power and the corresponding temperature. The figure shows that the second source produced approximately the same number of ions at almost 4(W) less power. This difference is again attributed to mounting and manufacturing differences. Figure 22 also shows that the two coated Potassium sources perform much the same when ion production is compared as a function of temperature.

##### *b, Temperature and Grid Potential*

Figure 24 shows the effect of varying the grid potential at various temperatures. It shows that for the first coated Potassium source an increase in temperature caused an increase in ion production at all extraction potentials. However, the second source produced less ions than the first source when operated at 20(°C) higher temperature. This difference is attributed to the fluctuation in current production observed with the coated Potassium sources.

## D. CESIUM ION SOURCE

Two Cesium ion sources were tested during these experiments. Both sources were used to exhaustion for the purpose of lifetime testing and verification of results.

### 1. Lifetime

The first Cesium source was slowly heated to 895(°C). Several grid and power sweeps were performed and then the heater power to the source was gradually increased to 1100(°C) over a period of days in an attempt to increase the lifetime of the source. The lifetime current production of the first source is shown in Figure 25. Current production fell to under 2( $\mu$ A) after 44 hours and 55 minutes of operation while the extraction potential was maintained at -100(V). The screen current of this sources varied as much as 3( $\mu$ A) in a matter of seconds throughout the lifetime of sources. The grid current remained relatively stable throughout the experiments. The fluctuation in current production is probably due to the low ionization of Cesium and the relatively high temperatures at which the source was operated. This source never produced more than 10( $\mu$ A) of current throughout its operation.

## 2. Power and Temperature

The heater power was slowly decreased after the source had been operated for several hours. Current production as a function of power and temperature for the first Cesium source is shown in Figure 26. Current production increased with increasing power and the source produced  $1(\mu\text{A})$  of current at below  $760(^{\circ}\text{C})$  and  $9.4(\text{W})$  power. The exact temperature is unknown because the lowest temperature reading possible on the optical pyrometer used was  $760(^{\circ}\text{C})$ .

## 3. Extraction Potential

Figure 27 shows the total current as a function of extraction grid potential for the first Cesium ion source. The grid potential was decreased from  $-100(\text{V})$  to  $-10(\text{V})$  while maintaining a constant temperature and a constant screen potential. This figure shows that Cesium ion production is increased with increased extraction potential with the sharpest increase occurring from  $-10(\text{V})$  to  $-40(\text{V})$ . This figure also shows that the screen current is initially greater than the grid current but flattens out at  $3(\mu\text{A})$ . The screen current and total current are average values of the current produced at any one time as the screen current varied as much as  $3(\mu\text{A})$  in a matter of seconds. The grid current was relatively stable. Again, this instability is

probably due to the low ionization energy of Cesium and the relatively high temperatures applied during these experiments.

#### 4. Cesium Source Comparison

##### *a, Lifetime*

Figure 28 shows the data from Figure 25 with the data from the second Cesium source added. The first source produced above  $2(\mu\text{A})$  of current for 44 hours and 55 minutes with an applied extraction potential of  $-100(\text{V})$ . The second source lasted only 27 hours. The second source was initially operated at a higher temperature and produced more current during that time which would account for the difference in lifetime between the two sources. The total ion production of the two sources over their entire lifetime was comparable.

##### *b, Power*

Figure 29 shows total current production of the two Cesium sources as a function of applied heater power and the corresponding temperature. The figure shows that the two sources performed relatively the same with respect to power and temperature.

##### *c, Temperature and Grid Potential*

Figure 30 shows the effect of varying the grid potential at various temperatures. It shows that for the

second source an increase in extraction potential causes an increase in ion production. This experiment was not run on the first Cesium source.

## E. CESIUM ION SOURCES WITH COATING

Two Cesium ion sources with Osmium-Ruthenium coating were tested for ion production. Both sources were used to exhaustion for the purpose of lifetime testing and verification of results.

### 1. Lifetime

The first coated Cesium source was slowly heated to 900(°C). The temperature was later increased to 925(°C) and the current production of the source declined throughout the experiment. Figure 31 shows the operating lifetime of the source. After 8 hours of operation the current production fell to below 2( $\mu$ A) and the source was removed from the ion gun. No grid extraction or power experiments were performed on this source because of its short lifetime. Throughout the life of the source the current production was unstable. The current varied as much as 2( $\mu$ A) in a matter of seconds. This fluctuation is probably due to the Osmium-Ruthenium coating and the low ionization energy of Cesium which caused inconsistent ion production in the current production range over which this source was operating.

## 2. Power and Temperature

The power to the heater of the first coated Cesium source was observed when the source was initially heated. Figure 32 shows the ion production for the first ion source as a function of power and temperature. The source produced  $1(\mu\text{A})$  of current below  $760(^{\circ}\text{C})$  and  $8(\text{W})$  of power. Ion production increased with temperature until  $900(^{\circ}\text{C})$ , which was the upper limit of the initial heating, without showing signs of flattening out.

## 3. Extraction Potential

Figure 33 shows the total current as a function of extraction grid potential for the second coated Cesium source. The grid potential was lowered from  $-200(\text{V})$  to  $-100(\text{V})$  while maintaining a constant temperature and screen potential. The figure shows that Cesium ion production is increased with increased extraction potential and the sharpest increase occurred from  $-10(\text{V})$  to  $-60(\text{V})$ . Figure 33 also shows that the grid current is always greater than the screen current and both currents increase at the same rate with increased extraction potential.

## 4. Coated Cesium Source Comparison

### *a, Lifetime*

Figure 34 shows the lifetime current production of the two coated Cesium sources. The first source produced currents above  $2(\mu\text{A})$  for 8 hours and 38 minutes while the

second source lasted for just over 14 hours. The first source was initially operated at higher temperatures and produced more ions during this time than the second source. This difference in source operation would account for the difference in lifetime. Therefore, the total ion production of the two sources are comparable.

*b, Power*

Figure 35 shows the total current production of the two coated Cesium sources as a function of applied heater power and the corresponding temperature. The figure shows that the two sources performed very differently with respect to power and temperature. The fluctuating current production and the differences in sources stated before contributed to these results.

## VII. SOURCE COMPARISON

For the purpose of comparison, a minimum requirement of  $10(\mu\text{A})$  of relatively stable current production is assumed to be necessary for the purposes of spacecraft charge control.

### A. SOURCE LIFETIMES

Of the five types of sources tested, a Lithium source produced ions for more than twice as long (93 hours) as the next best sources. Only one Lithium source was operated to exhaustion but the second Lithium source was operated for over 43 hours without falling below  $2(\mu\text{A})$  of current production. The Potassium sources and the Cesium sources both lasted approximately 44 hours. The coated Potassium source lasted almost as long as the uncoated Potassium source and fell below the  $2(\mu\text{A})$  cutoff after 38 hours. The coated Cesium sources had the shortest lifetimes and fell below the cutoff after only 14 hours of ion production. Therefore, Lithium would be judged the best source type in the criteria of lifetime based on the results of these experiments. Potassium, Cesium, and coated Potassium sources would be judged as equal second best choices in the lifetime criteria.

The percentage of alkali ions extracted from the exhausted sources could not be estimated from these experiments. There is an unknown loss of the alkali material, due to evaporation and surface preparation, during the manufacturing process. Detailed measurements would have to be taken at all stages of production in order to estimate the percentage of alkali material extracted as ions.

## B. POWER AND TEMPERATURE

It is advantageous to produce a sufficient quantity of ions to control spacecraft charging at the lowest possible temperature and therefore at the lowest required power. This fact is based on the limited power available on operating satellites. For this reason, lower temperature current production will be judged as better.

### 1. Coated and Uncoated Sources

#### *a, Potassium*

Figure 36 shows a comparison of the coated and uncoated Potassium sources current production as a function of temperature. At lower temperatures the coated Potassium source produced approximately the same current as the uncoated source at more than 50(°C) lower temperature. This relationship holds until the current production coincides at approximately 940(°C). The reduction in temperature requirement is due to the Osmium-Ruthenium coating's higher

surface work function. Therefore, in respect to temperature and required power the coated Potassium would be judged to be the better source.

### *b, Cesium*

Figure 37 shows a comparison of the coated and uncoated Cesium sources current production as a function of temperature. At lower temperatures the coated Cesium source produced more current than the uncoated source until the sources reached 790(°C) where the coated Cesium source's current production fell below that of the uncoated source. For the purpose of charge control, the coated Cesium sources produced insufficient currents at all temperatures. None of the coated Cesium ion sources reached the desired current production level of 10( $\mu$ A) at any time during any of the experiments that were conducted. Although the coated source does initially produce current at lower temperatures than the uncoated source, this current is insufficient for the purposes of charge control and the uncoated Cesium ion source is judged to be the better source with respect to temperature and power requirements.

## 2. All Sources

Figure 38 shows a comparison of all the types of ion sources examined with respect to temperature. The Lithium source did not produce 10( $\mu$ A) of current until it reached 1050(°C) which is was 150(°C) higher than the next closest

type of ion source. This temperature difference is due to the higher ionization energy of Lithium as compared to Potassium and Cesium. Figure 39 shows the same comparison with the Lithium source removed. The Potassium ion source required a temperature of 910(°C) to reach the 10( $\mu$ A) level. The Cesium ion source reached the same level at 865(°C) while the coated Potassium source required only 850(°C) to reach 10( $\mu$ A) of current production. The coated Cesium ion source never reached the 10( $\mu$ A) level at any of the temperatures applied. The figure therefore shows that the Osmium-Ruthenium coating on the surface of the coated Potassium source is able to overcome the expected lower temperature requirements of Cesium due to its lower ionization energy. Therefore, based on these experiments the coated Potassium ion source would be judged to be the better ion source type with respect to power and temperature requirements.

### C. EXTRACTION POTENTIAL

Figure 40 shows the total current as a function of extraction grid potential for each type of ion source. All of the sources were initially set at a power and corresponding temperature so that the current production was a constant 10( $\mu$ A) with an applied extraction potential of -100(V) and a screen current of -200(V). The coated Cesium

source never reached  $10(\mu\text{A})$  as the figure shows. The extraction grid was then increased to  $-200(\text{V})$  and slowly decreased to  $-10(\text{V})$ . The figure shows that the Lithium ion source was the most effective ion producer at lower extraction potentials, closely followed by the Cesium ion source. However, both of the Potassium ion source types are more affected by extraction potentials greater than  $-100(\text{V})$ . This result indicates that the extraction potential required for ion production may be related to the mass of the extracted ions. It is possible that the larger Potassium atoms encounter a higher resistance in the lattice structure of the Beta-Eucryptite which can be overcome with an increase in the extraction potential. This hypothesis is substantiated to a certain degree by the Lithium ion source, which is producing smaller Lithium ions, reaching a constant current production at  $-50(\text{V})$ . These results suggest that the Potassium ion sources could be operated at lower temperatures with increased extraction potentials and produce sufficient ions for the purposes of charge control at lower power requirements. Further experiments, such as lifetime tests run at  $-200(\text{V})$  extraction potential, would have to be performed to verify the feasibility of this arrangement.

## VIII. CONCLUSIONS

The experiments performed in conjunction with this thesis evaluated Lithium, Potassium, Osmium-Ruthenium coated Potassium, Cesium, and Osmium-Ruthenium coated Cesium ion sources for possible use in satellite charge control devices. A comparison of these sources shows that only the Lithium and Potassium ion sources are acceptable for satellite charge control purposes. The choice between these two source types would be a trade off between the longer lifetime of the Lithium source and the lower power requirements of the Potassium source. The choice between these two sources would depend on the satellite charge control requirements and the number of sources which could be used in sequence in a charge control device.

These experiments showed that the idea of using Potassium sources in place of the Lithium sources does lower the power requirements for ion production in the emitter design used in these experiments. The experiments also showed that, although coating the sources to increase the surface work function does reduce the power requirements, the coated sources were unsuitable for use in charge control devices due to fluctuating current production.

# APPENDIX

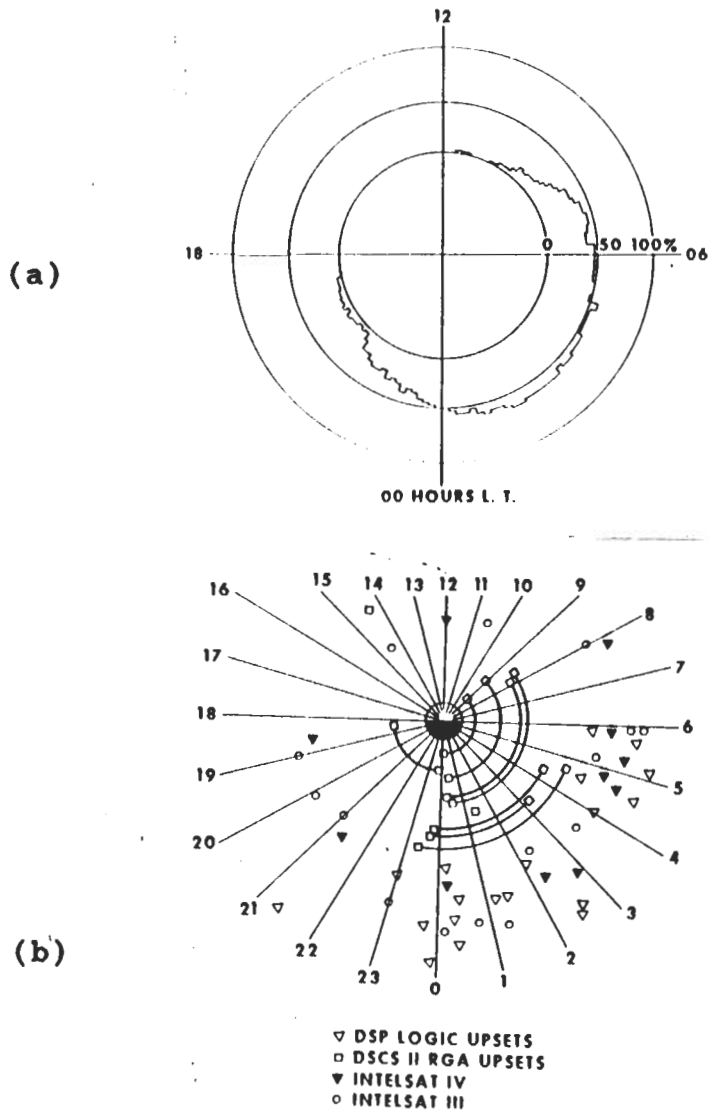


**Figure 1 (a). Time Distribution of ATS-6 Spacecraft Charging Events: probability that charging occurred plotted at the local time of the satellite. (b). Time Distribution of Spacecraft Anomalies: plotted at the local time of various satellites at geosynchronous orbit. [Ref.10]**

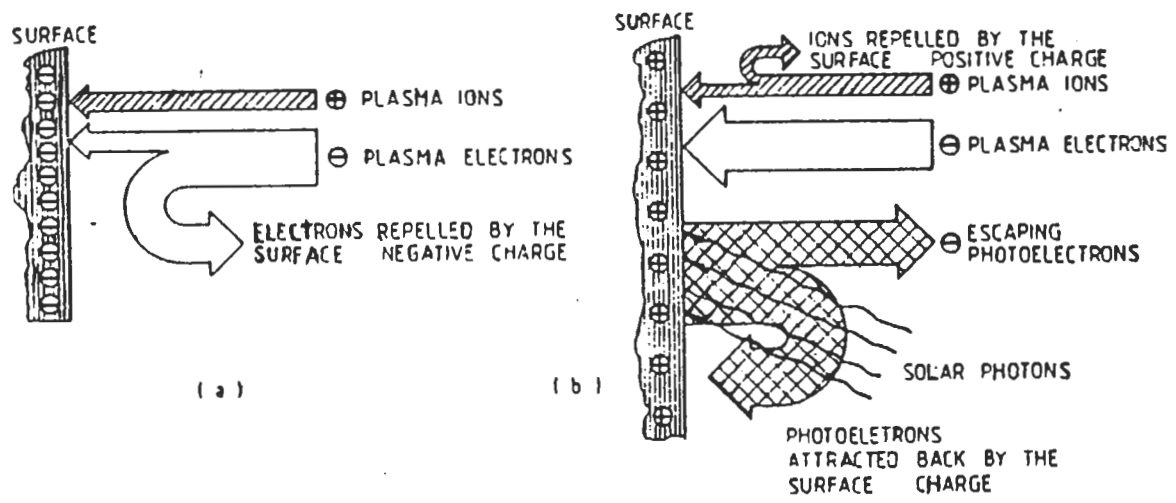


Figure 2 (a). Surface Charging in Shadow.  
 (b). Surface Charging in Sunlight.[Ref.12]

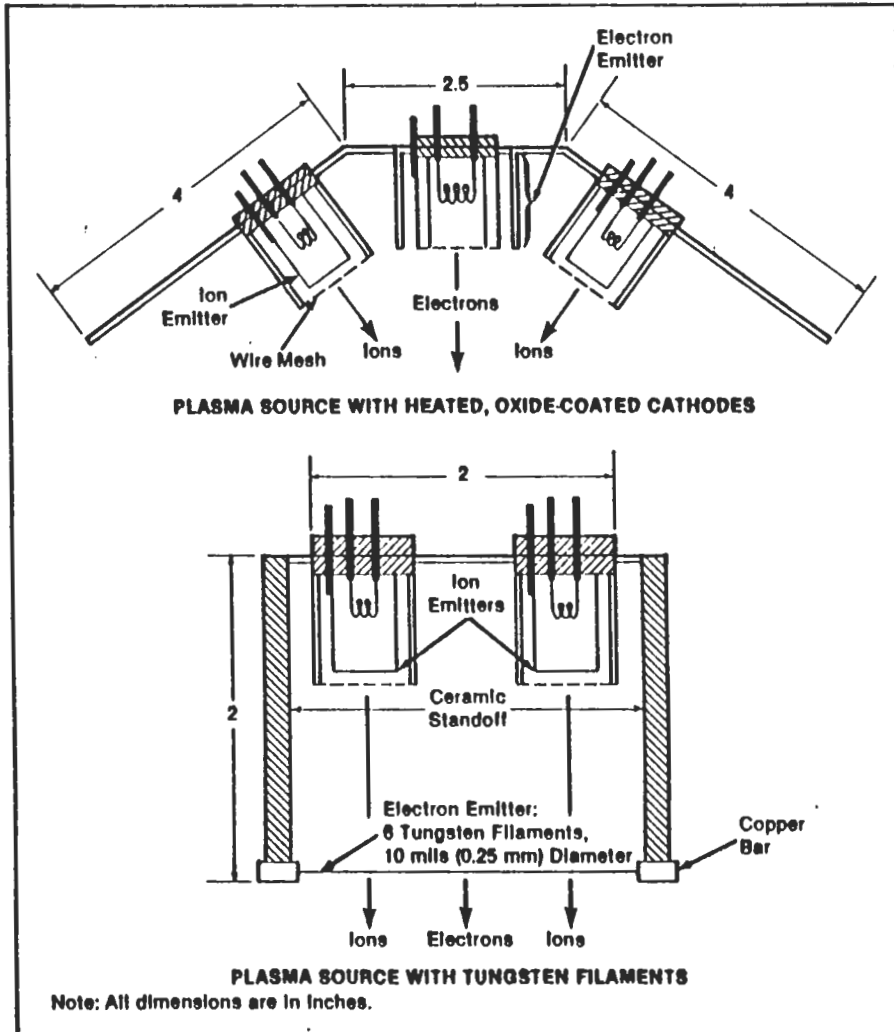


Figure 3. Plasma Source.[Ref.17]

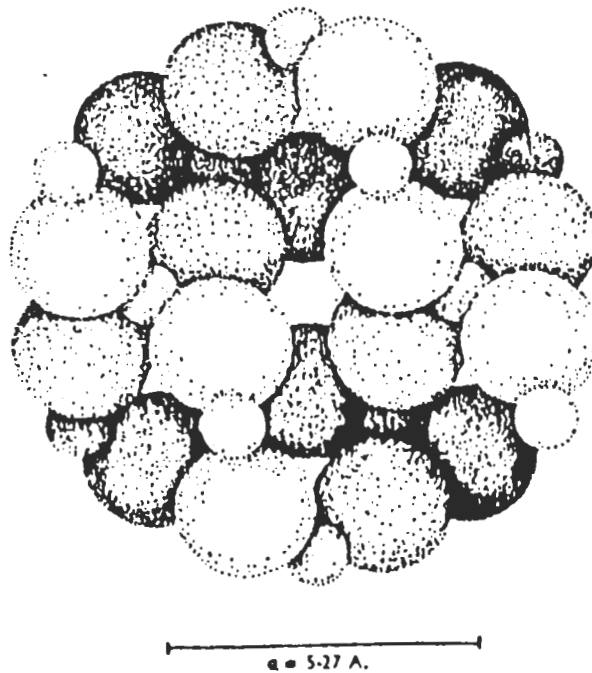
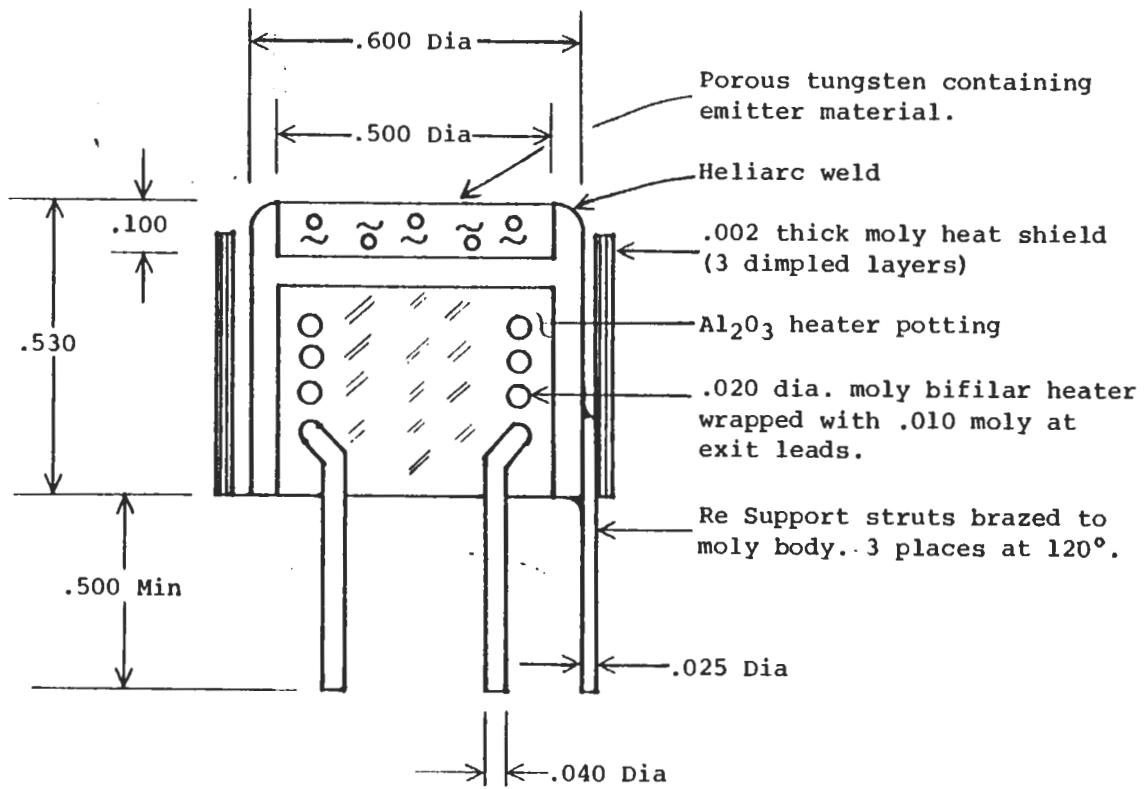
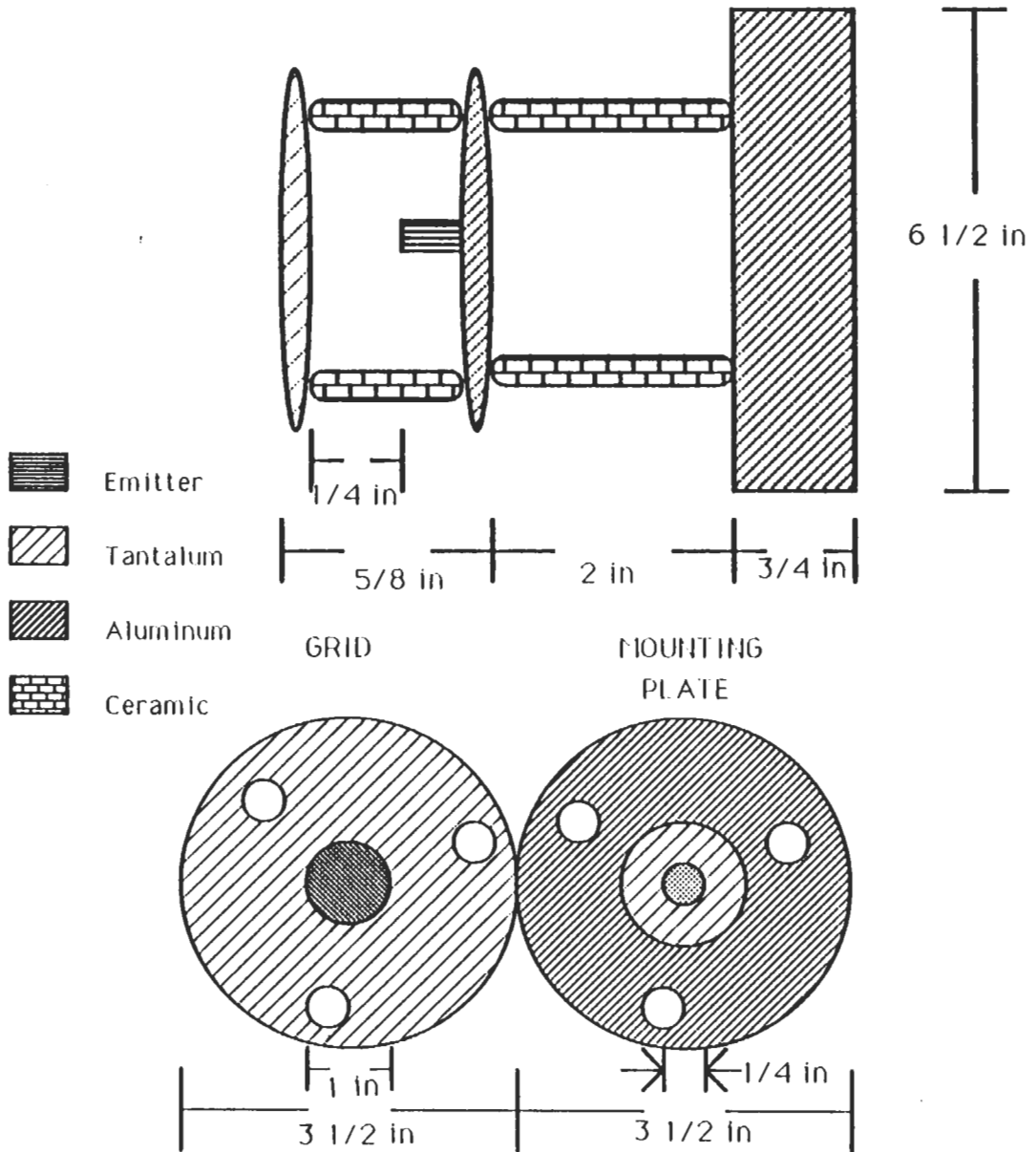


Figure 4. Crystal Structure of Beta-Eucryptite viewed along c axis. Large spheres represent oxygen atoms, small spheres either Si or Al atoms. The Lithium ions are situated in center openings.[Ref.21]



**Figure 5. Ion Source.** All dimension are in inches. The sources used were proportionally smaller with a diameter of .25 inches.[Ref.24]

# ION GUN



**Figure 6. Ion Gun.**

Electrical Diagram

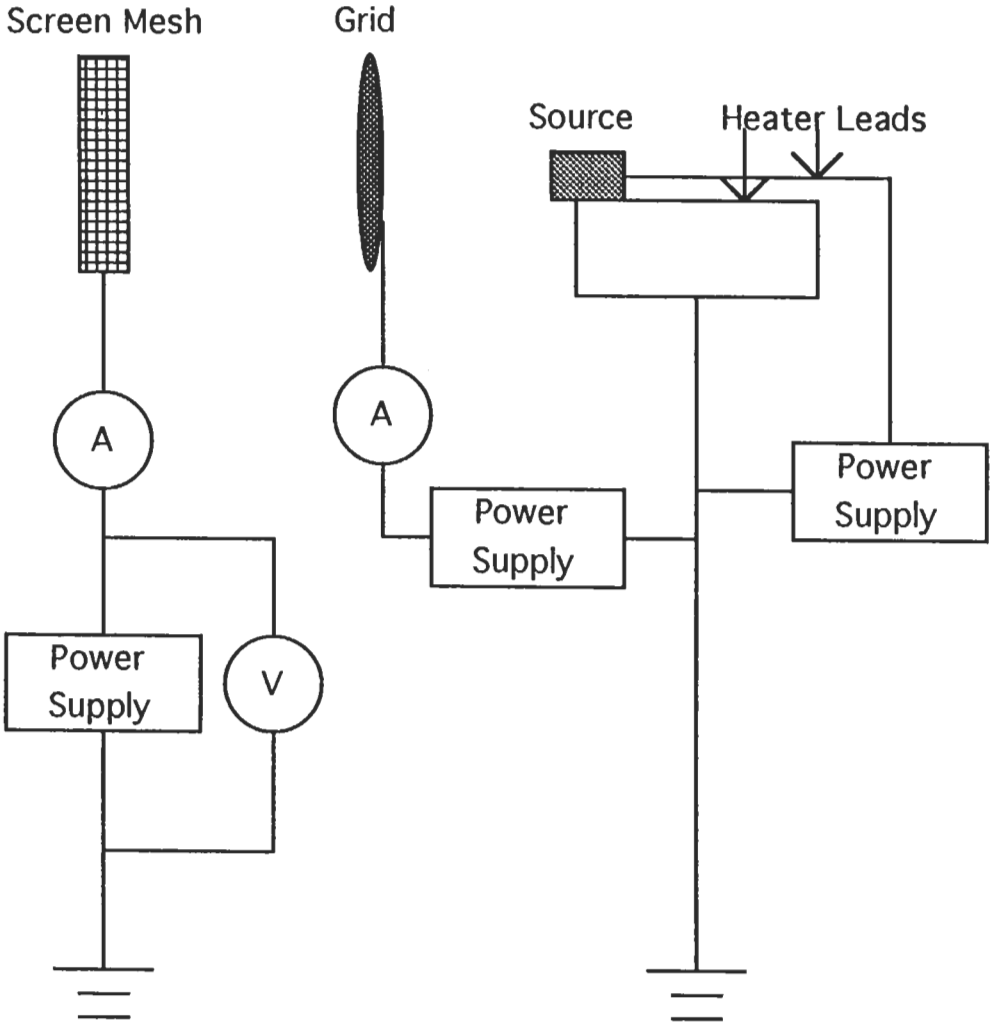


Figure 7. Electrical Wiring Diagram.

# LITHIUM LIFETIME

SCREEN - 200 V  
GRID - 100 V  
POWER RANGE (0 - 29.29) W

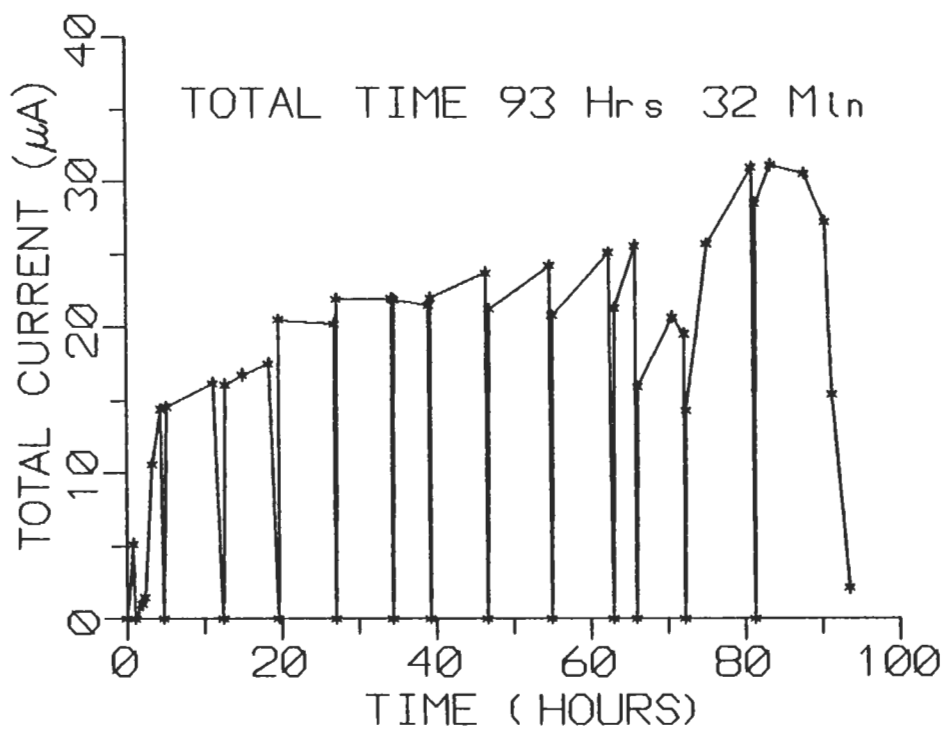


Figure 8. Lithium Lifetime.

# LITHIUM LIFETIME

TOTAL TIME 93 Hrs 32 Min

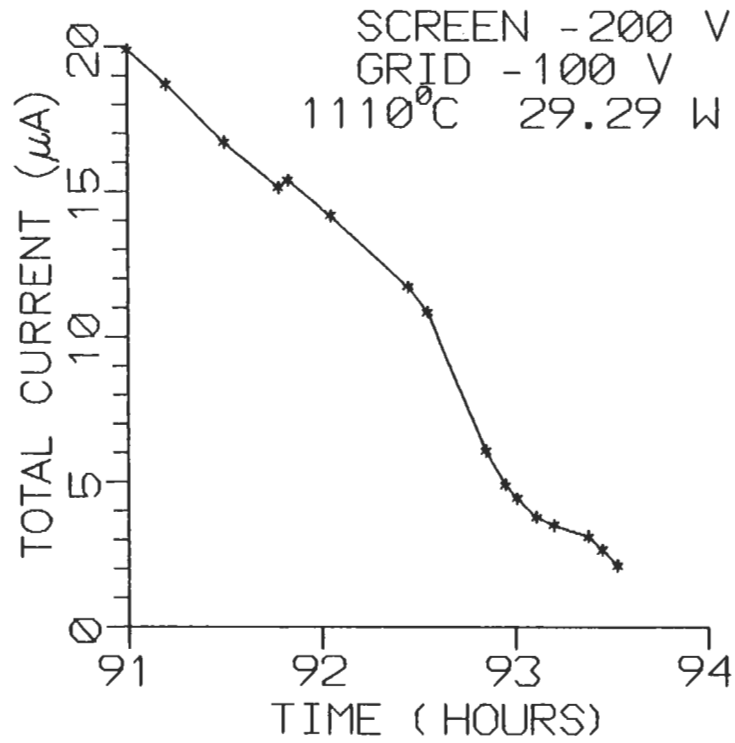


Figure 9. Final Hours of Lithium Lifetime.

# LITHIUM

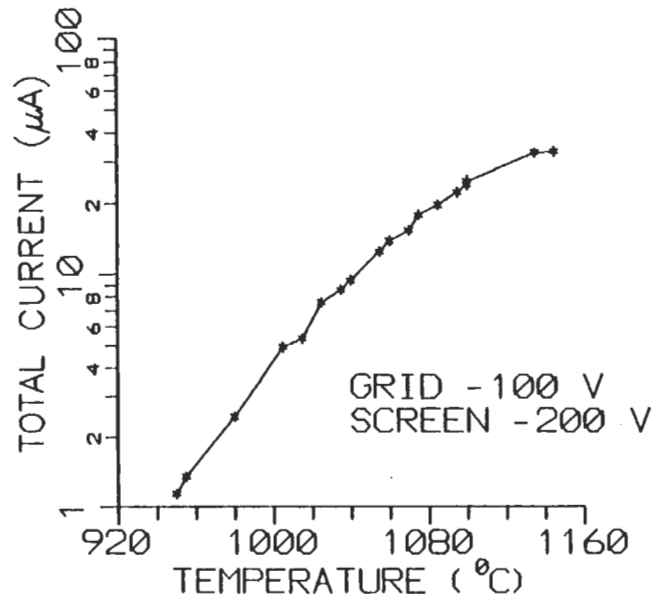
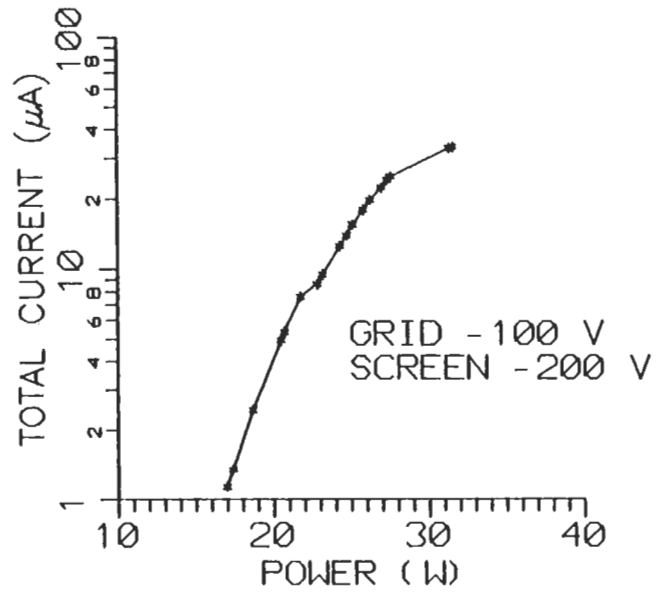


Figure 10. Lithium Total Current vs Power and Temperature.

# LITHIUM

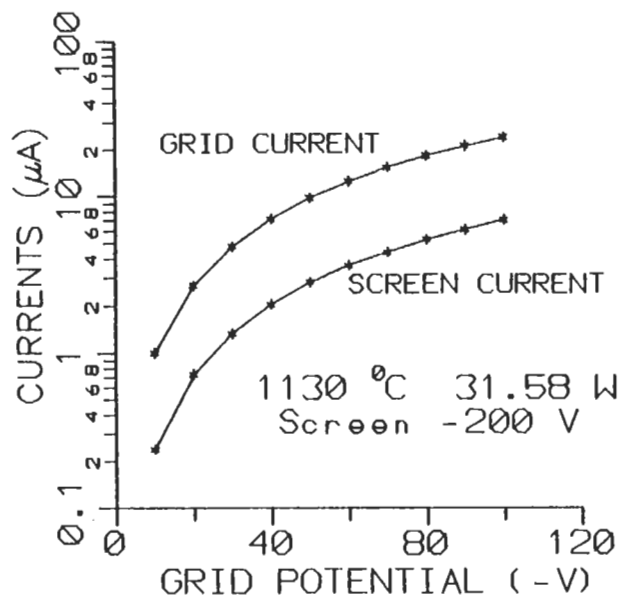
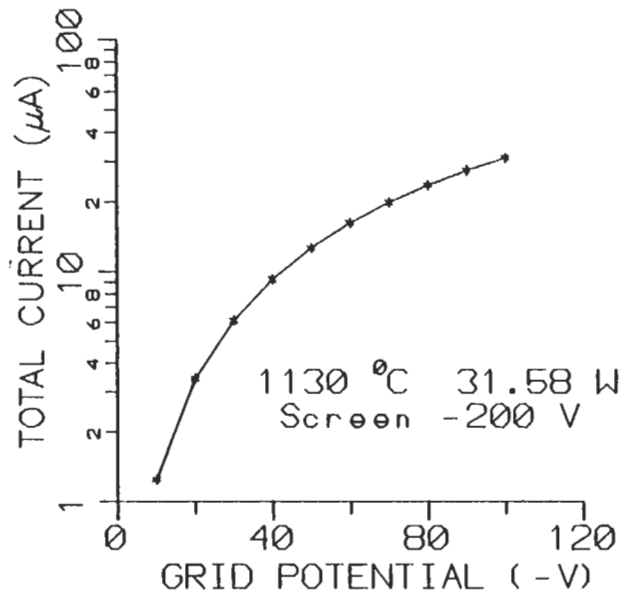


Figure 11. Lithium Total, Grid, and Screen Current vs Grid Potential.

# LITHIUM

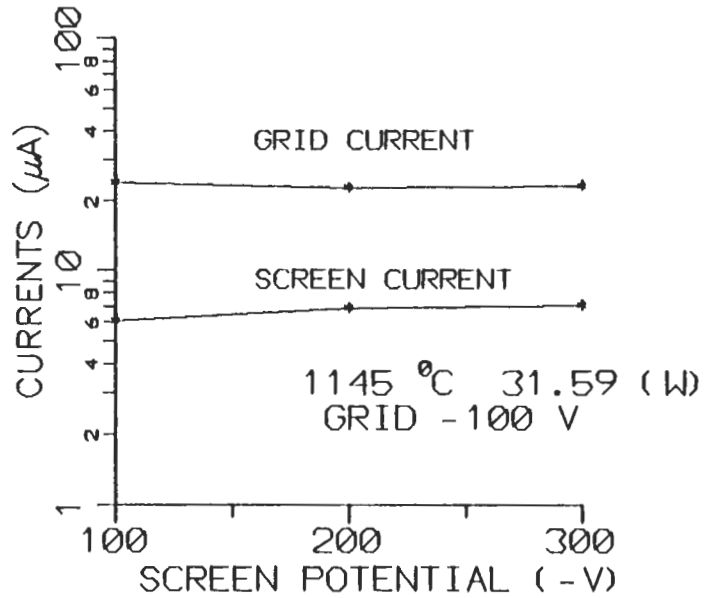
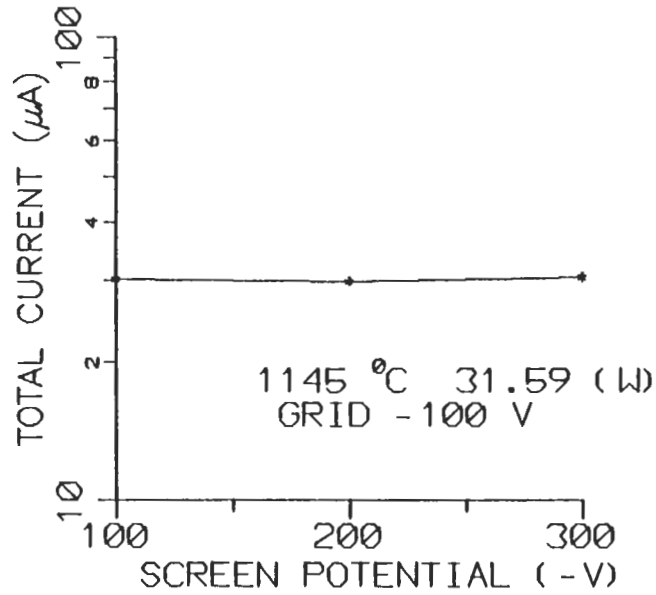


Figure 12. Lithium Total, Grid, and Screen Current vs Screen Potential.

# LITHIUM

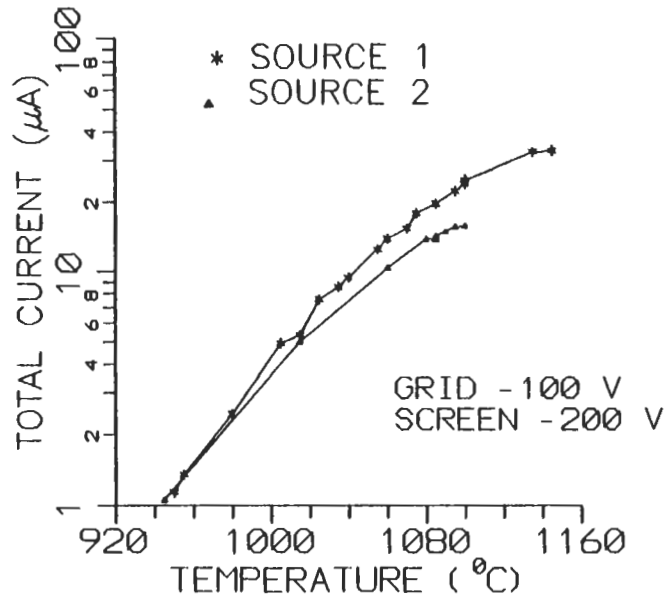
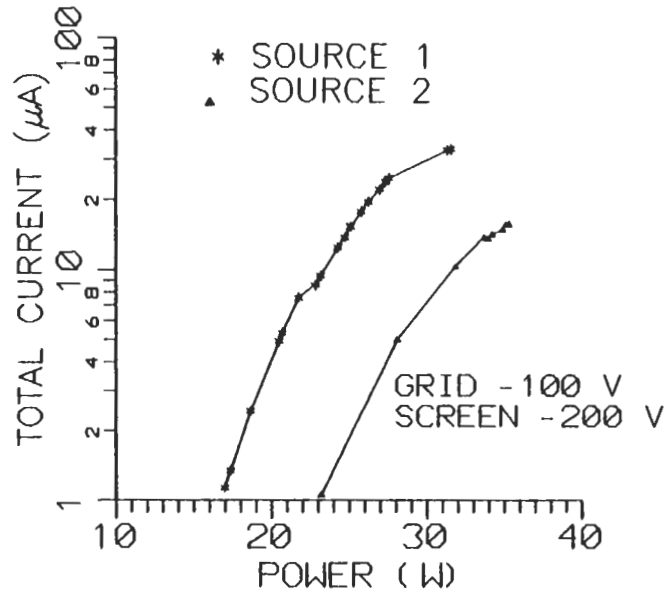


Figure 13. Lithium Total Current vs Power and Temperature.

# LITHIUM

\* SOURCE 1 1130 °C 31.58 W  
★ SOURCE 1 1100 °C 24.88 W  
▲ SOURCE 2 1085 °C 33.64 W

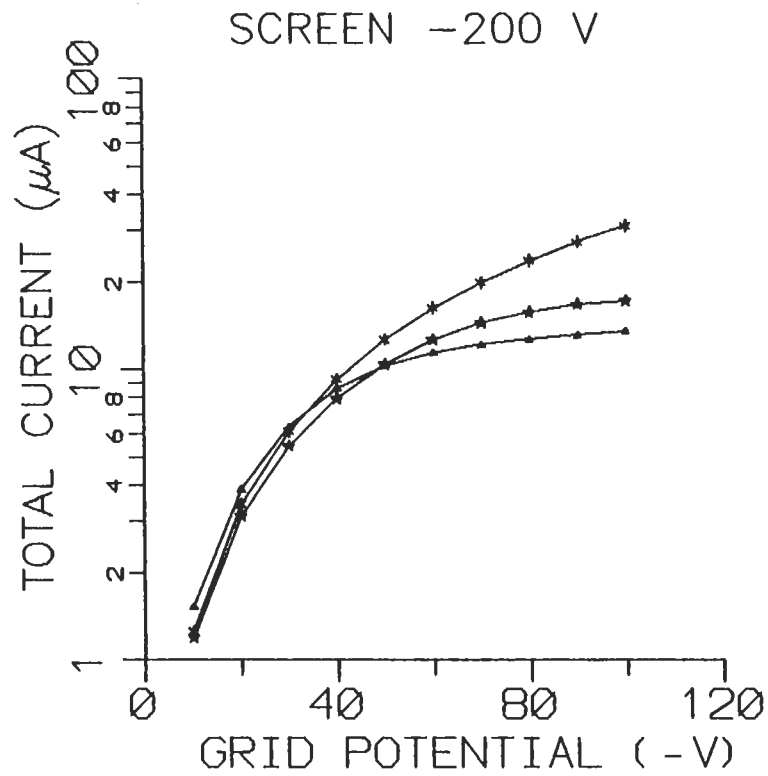


Figure 14. Temperature Variation Affects on Lithium Total Current vs Grid Potential.

# POTASSIUM LIFETIME

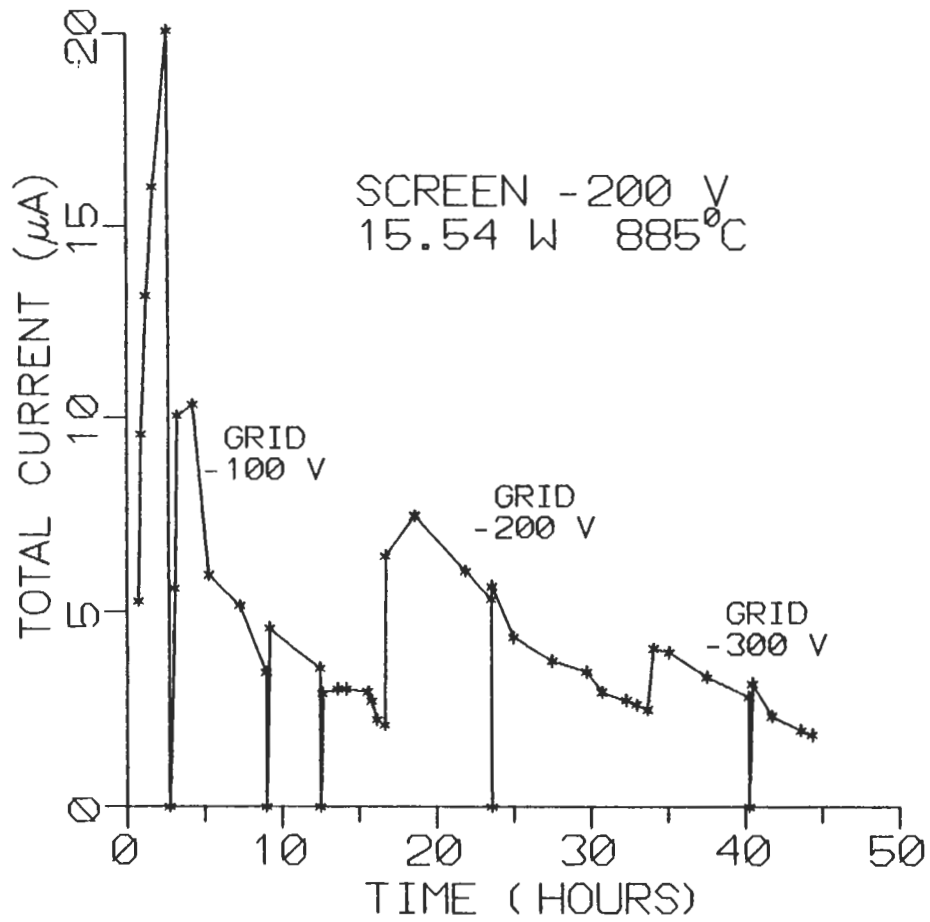


Figure 15. Potassium Lifetime.

# POTASSIUM

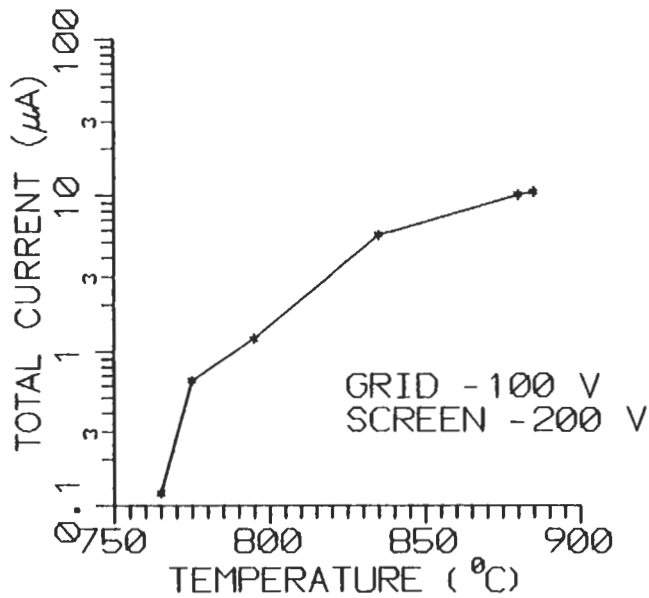
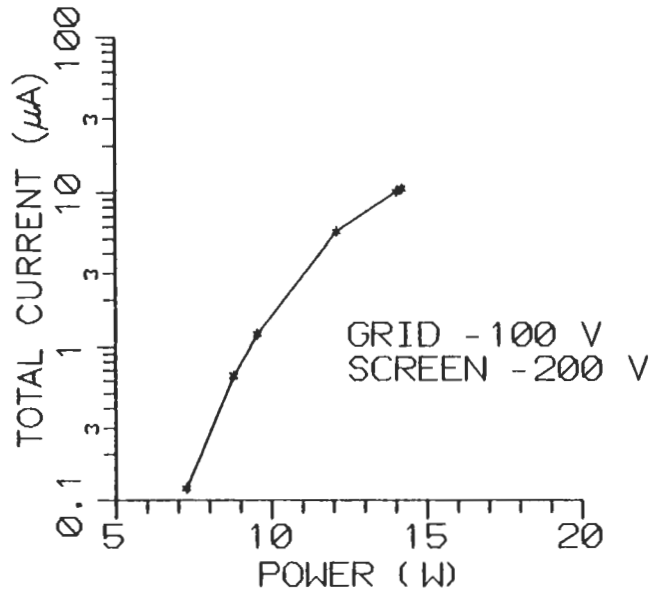


Figure 16. Potassium Total Current vs Power and Temperature.

# POTASSIUM

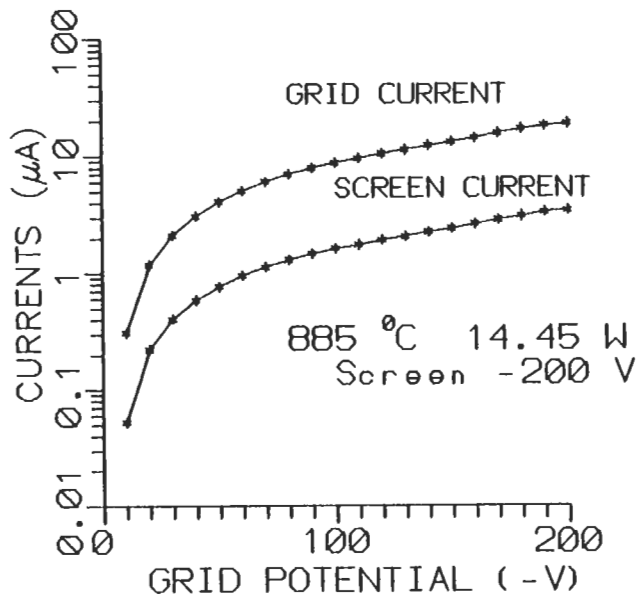
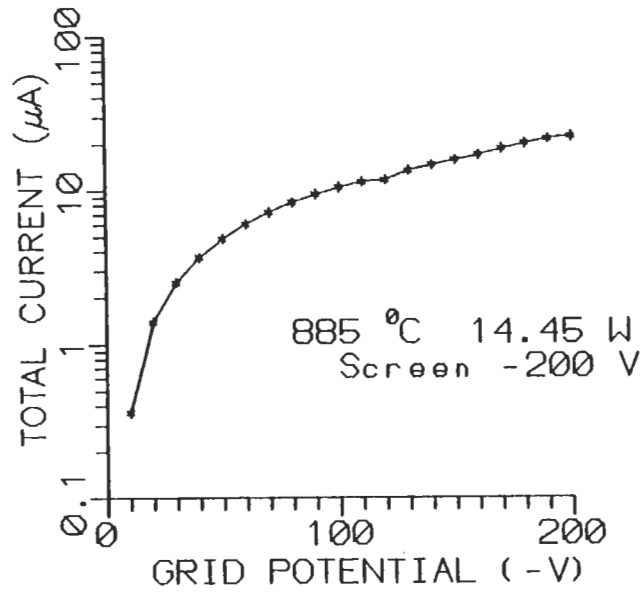


Figure 17. Potassium Total, Grid, and Screen Current vs Grid Potential.

# POTASSIUM LIFETIME

\* Source 1  
▲ Source 2

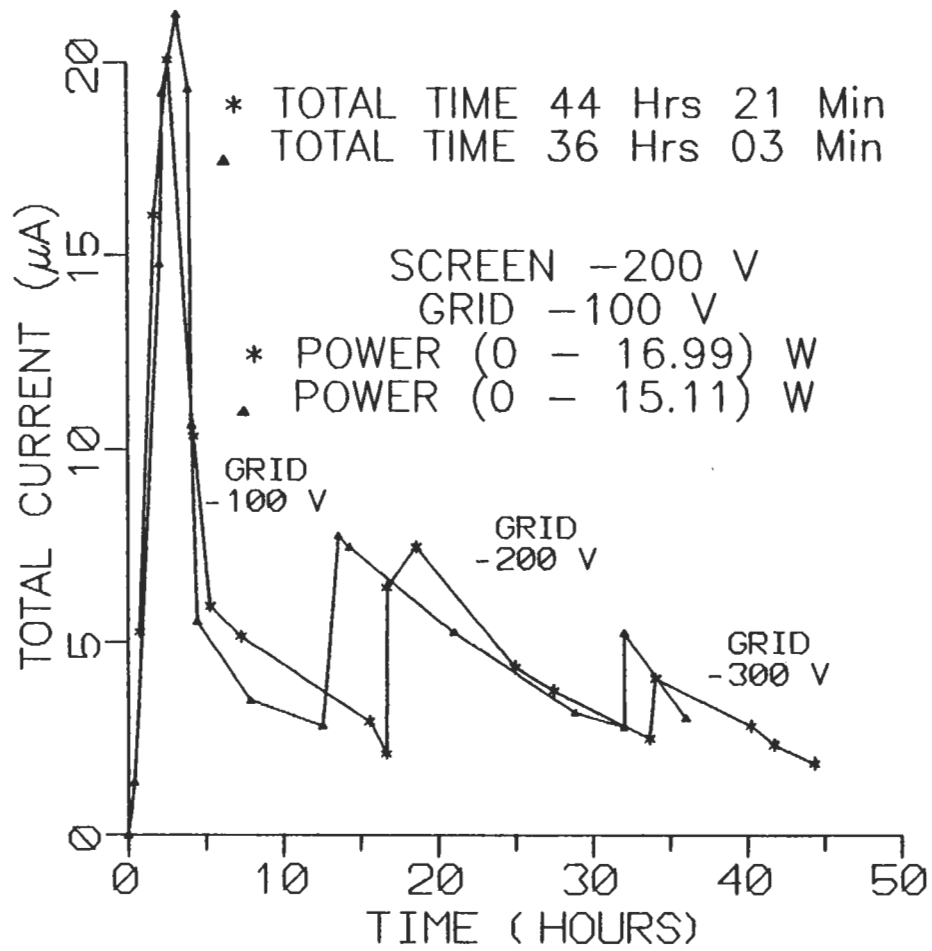


Figure 18. Potassium Lifetimes.

# POTASSIUM

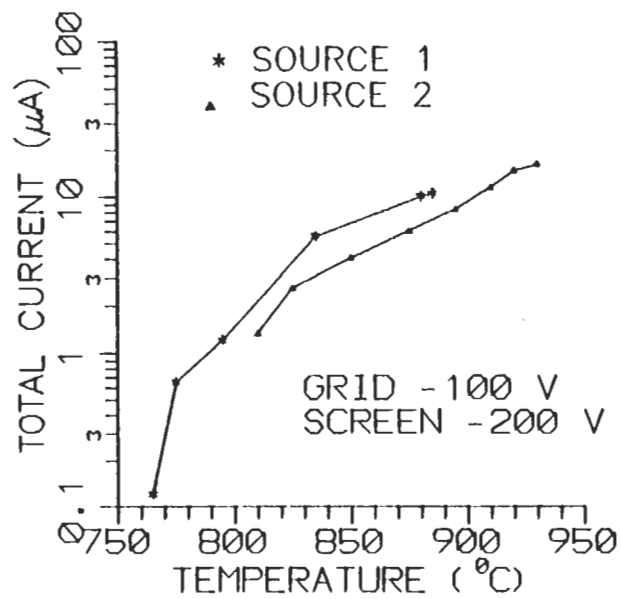
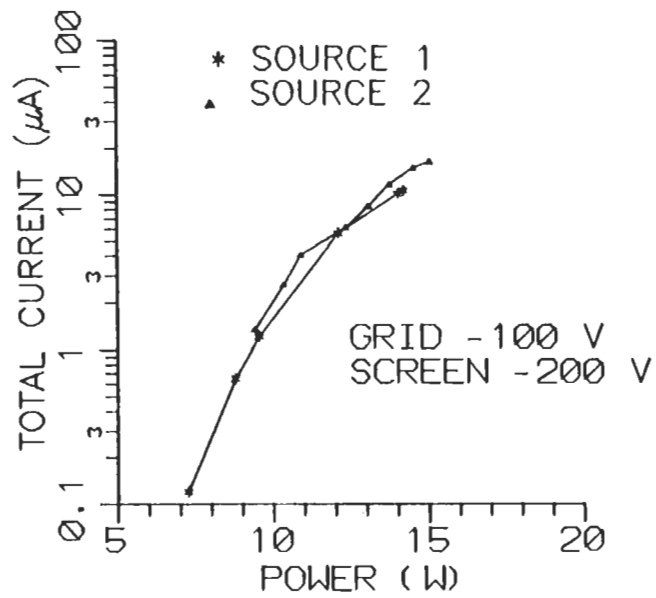


Figure 19. Potassium Total Current vs Power and Temperature

# POTASSIUM

\* SOURCE 1 885°C 14.45 W  
▲ SOURCE 2 925°C 15.11 W  
★ SOURCE 2 840°C 11.48 W

SCREEN -200 V

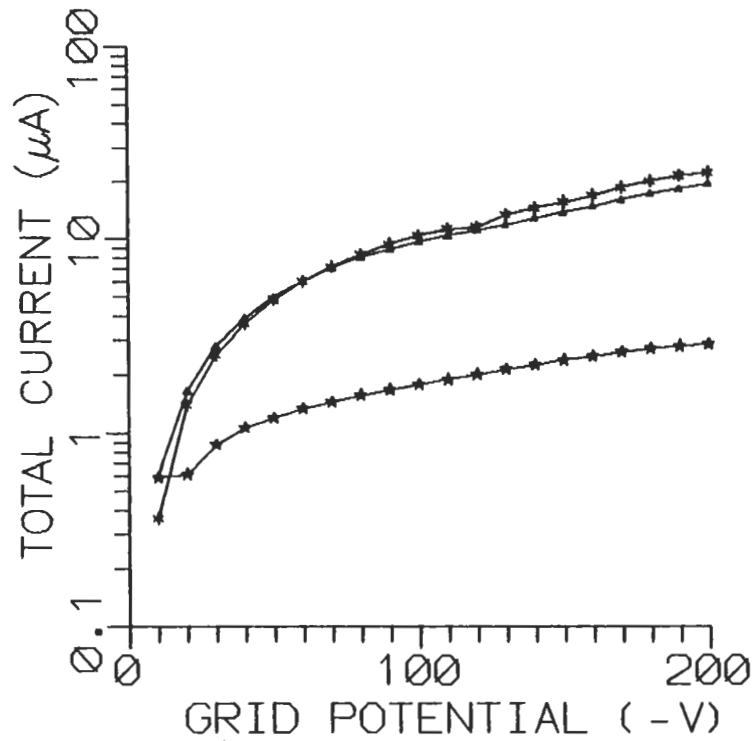


Figure 20. Temperature Variation Affects on Potassium Total Current vs Grid Potential.

# POTASSIUM LIFETIME WITH COATING

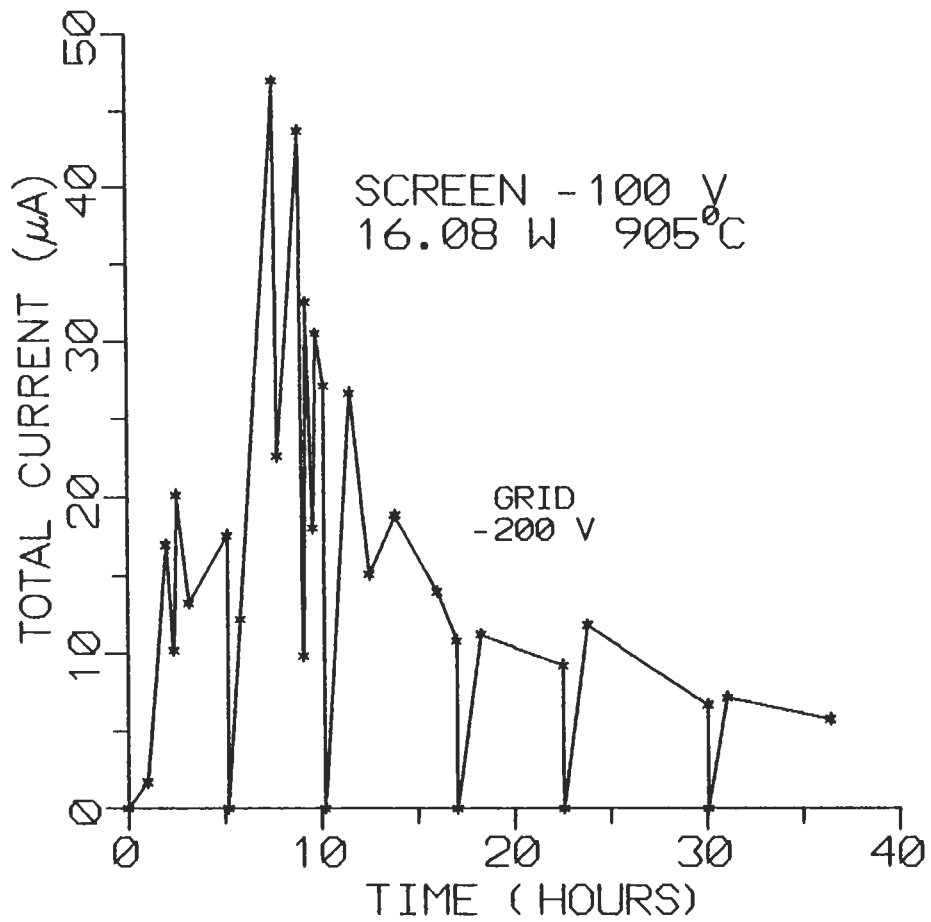


Figure 21. Potassium Lifetime With Coating.

# POTASSIUM WITH COATING

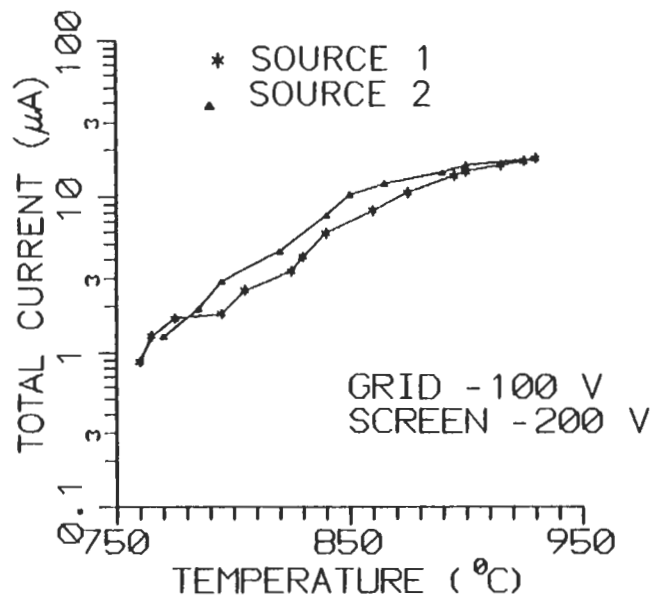
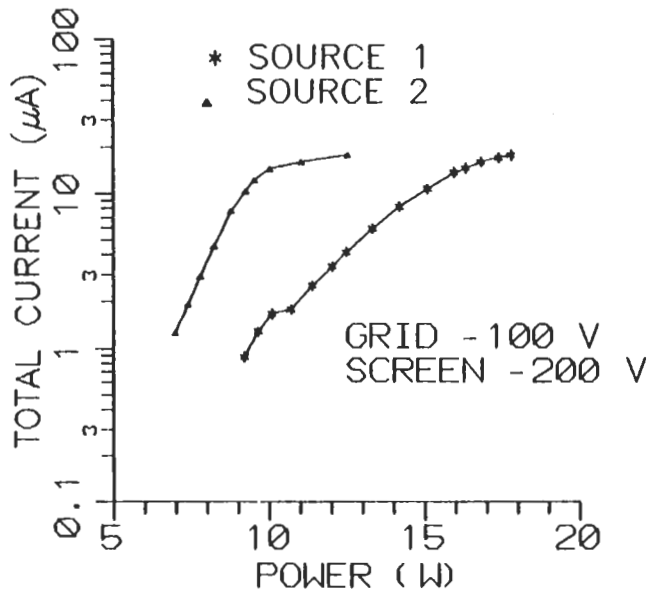


Figure 22. Potassium With Coating Total Current vs Power and Temperature.

# POTASSIUM WITH COATING

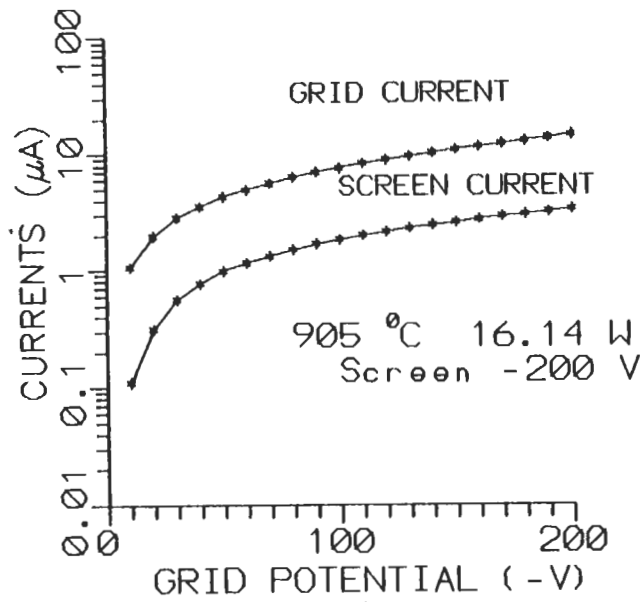
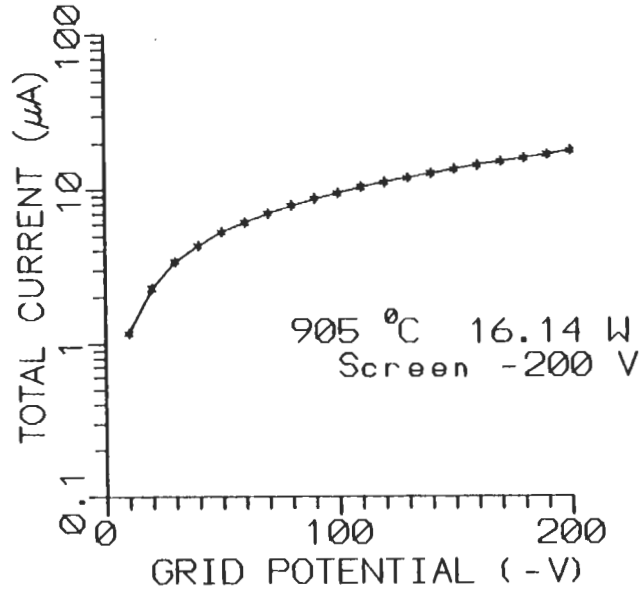
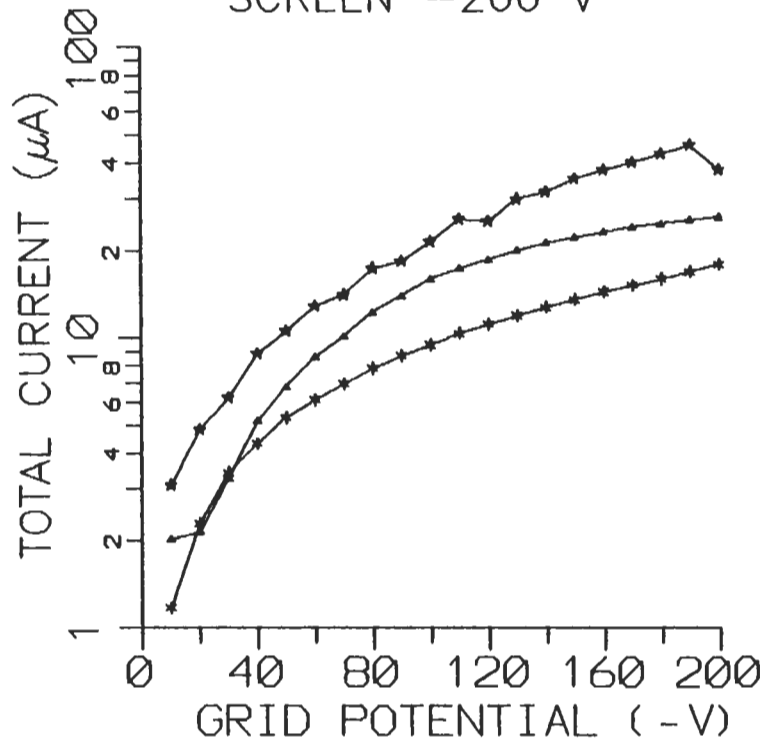


Figure 23. Potassium With Coating Total, Grid, and Screen Current vs Grid Potential.

# POTASSIUM WITH COATING

\* SOURCE 1 905 °C 16.14 W  
 ★ SOURCE 1 910 °C 16.64 W  
 ▲ SOURCE 2 925 °C 12.09 W

SCREEN -200 V



**Figure 24. Temperature Variation Affects on Potassium With Coating Total Current vs Grid Potential.**

# CESIUM LIFETIME

SCREEN -200 V  
GRID -100 V  
POWER RANGE (0 - 28.17) W

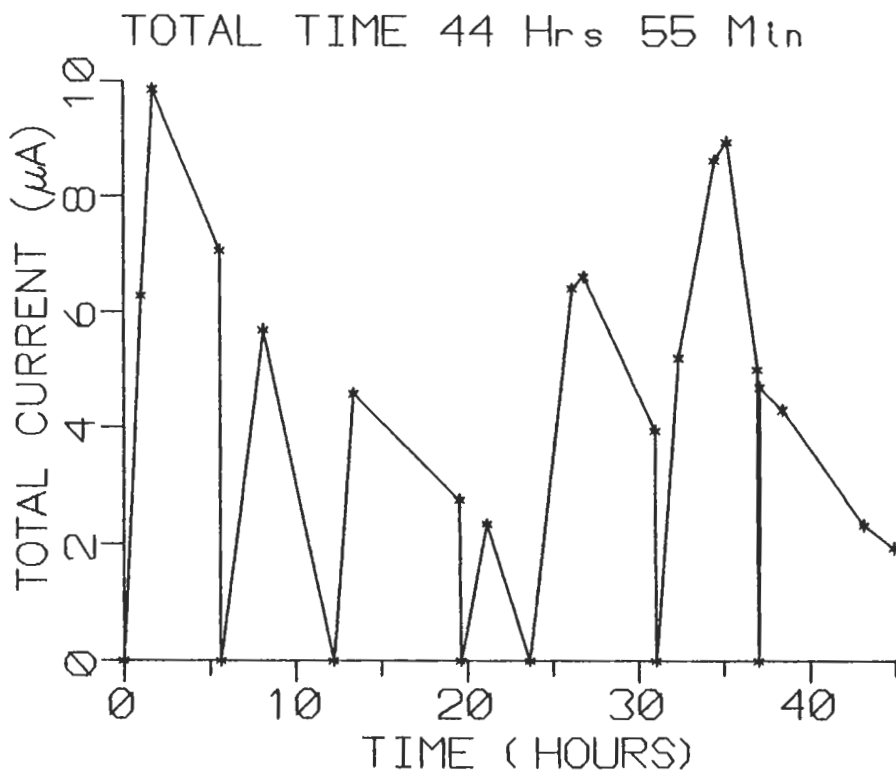


Figure 25. Cesium Lifetime.

# CESIUM

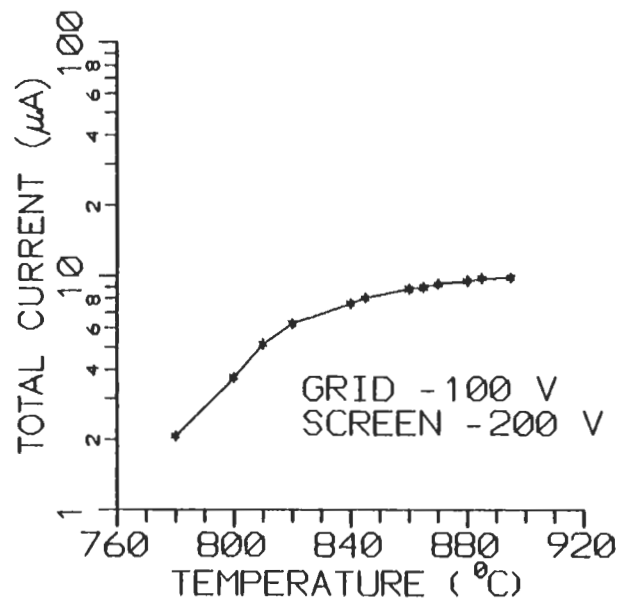
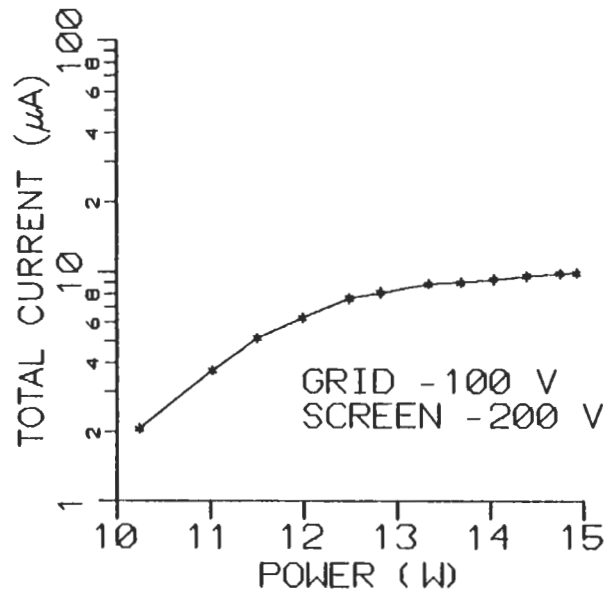


Figure 26. Cesium Total Current vs Power and Temperature.

# CESIUM

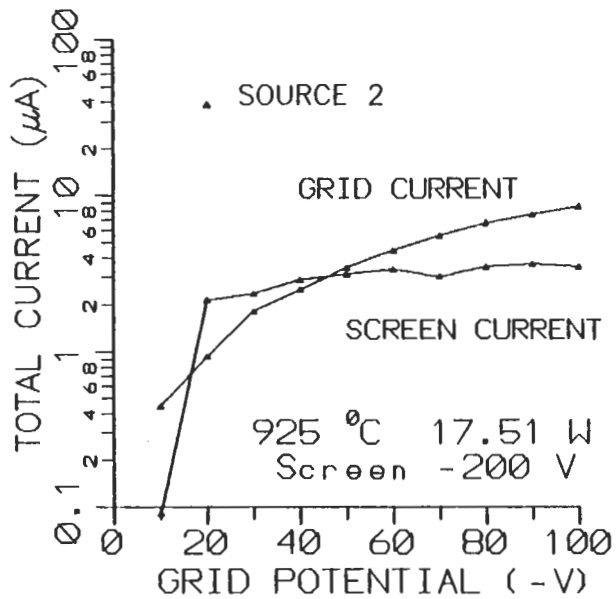
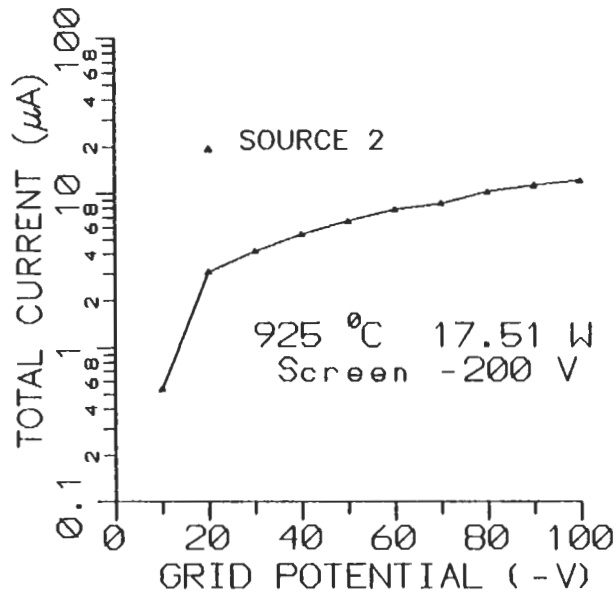


Figure 27. Cesium Total, Grid, and Screen Current vs Grid Potential.

# CESIUM LIFETIME

- \* Source 1
- ▲ Source 2

- \* TOTAL TIME 44 Hrs 55 Min
- ▲ TOTAL TIME 27 Hrs 01 Min

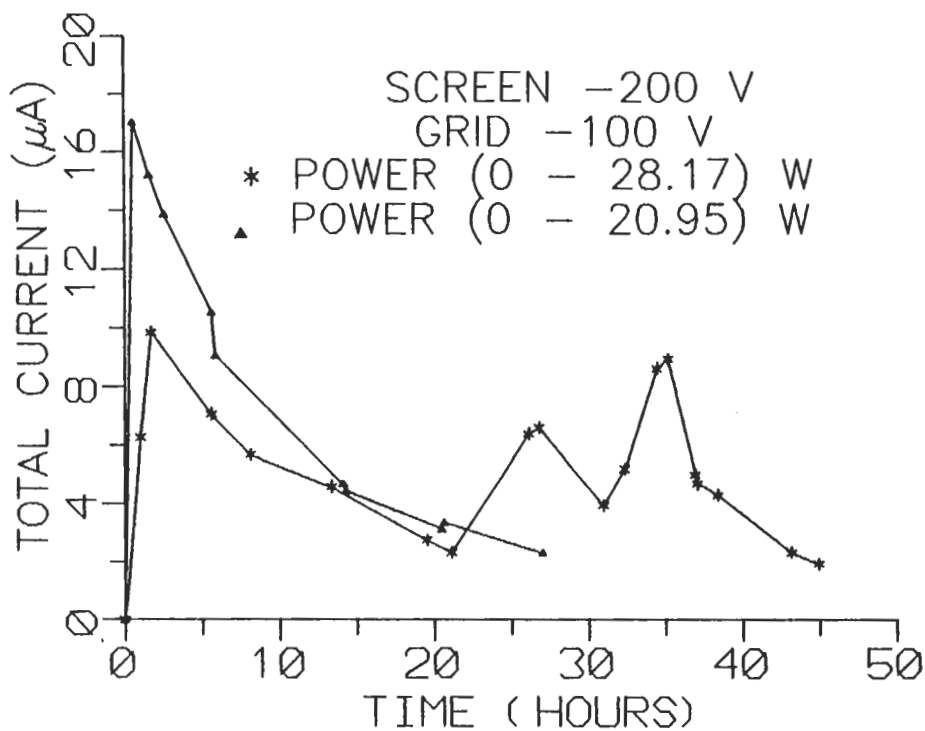


Figure 28. Cesium Lifetimes.

CESIUM

- \* Source 1
- ▲ Source 2

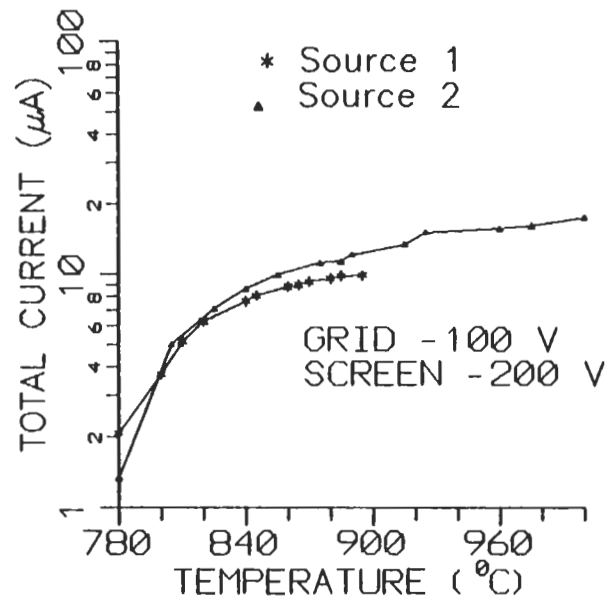
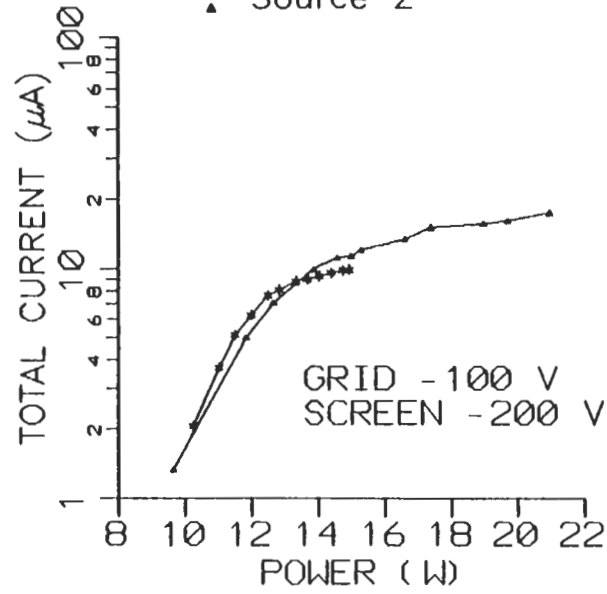


Figure 29. Cesium Total Currents vs Power and Temperature.

# CESIUM

▲ SOURCE 2 925<sup>0</sup>C 17.51 W  
★ SOURCE 2 990<sup>0</sup>C 20.32 W

SCREEN -200 V

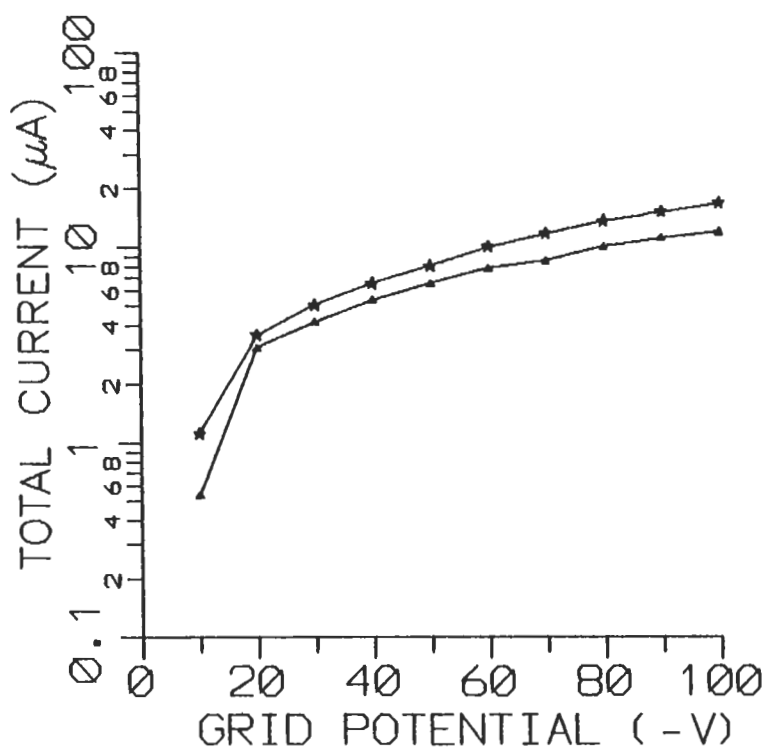


Figure 30. Temperature Variation Affects on Cesium Total Current vs Grid Potential.

# CESIUM LIFETIME WITH COATING

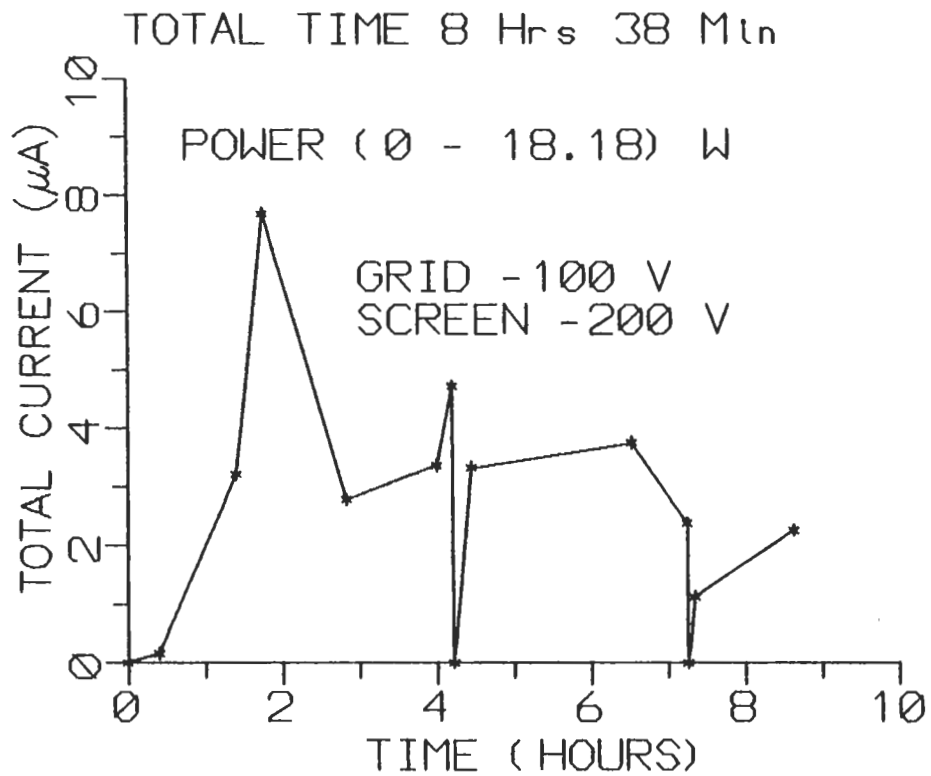


Figure 31. Cesium Lifetime With Coating.

CESIUM  
WITH COATING

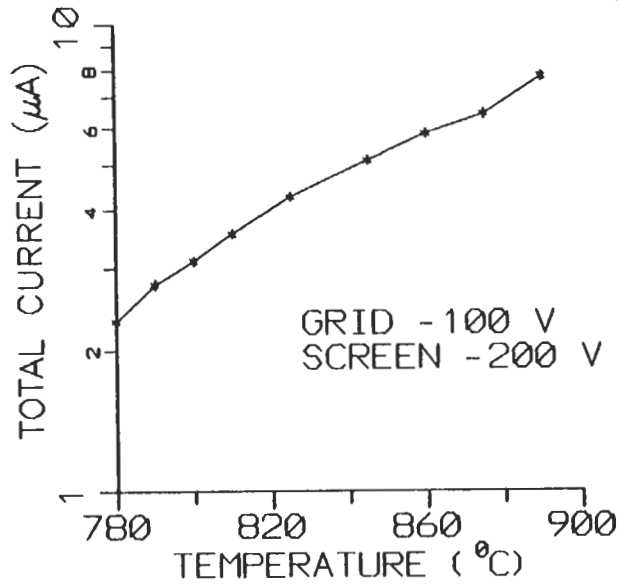
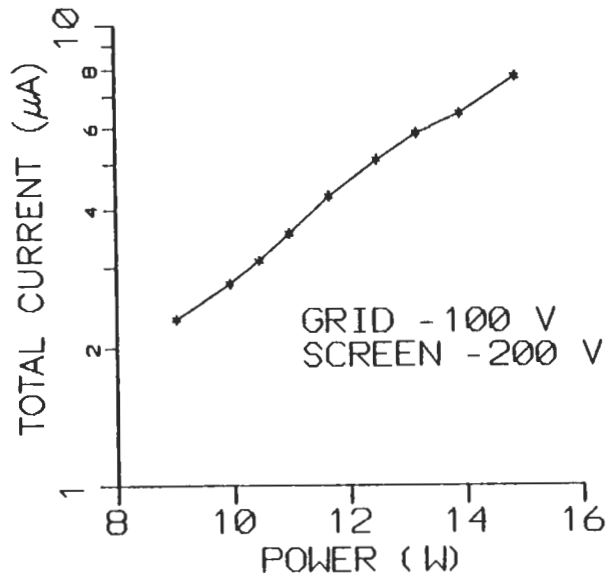


Figure 32. Cesium With Coating Total Current vs Power and Temperature.

CESIUM  
WITH COATING

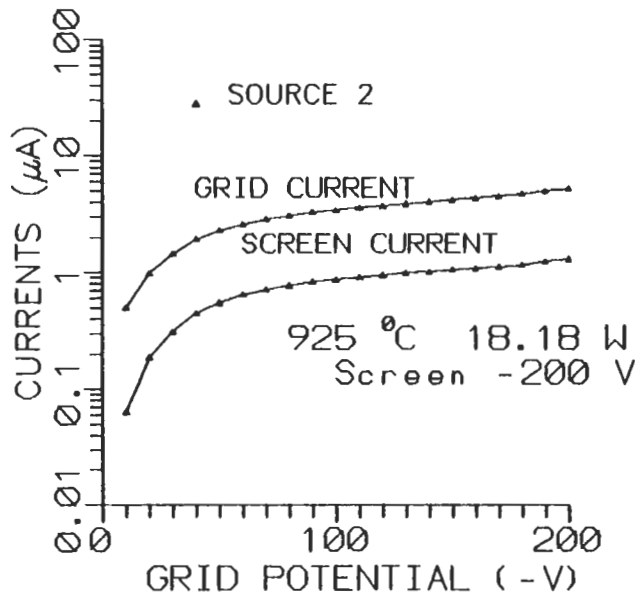
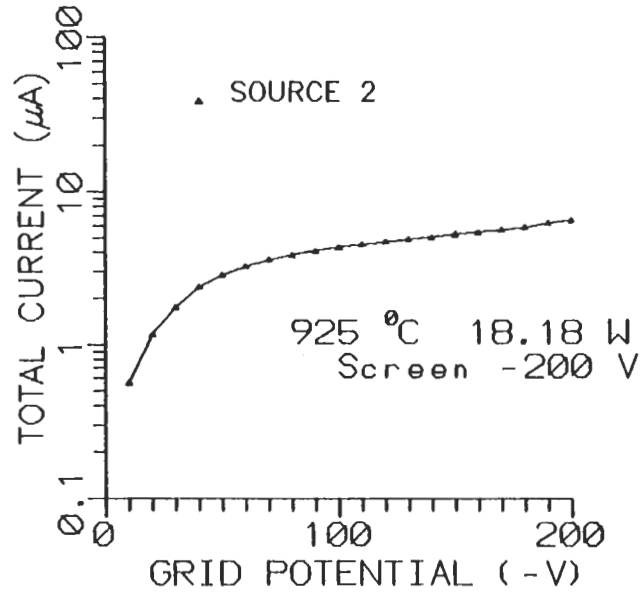


Figure 33. Cesium With Coating Total, Grid, and Screen Current vs Grid Potential.

# CESIUM LIFETIME WITH COATING

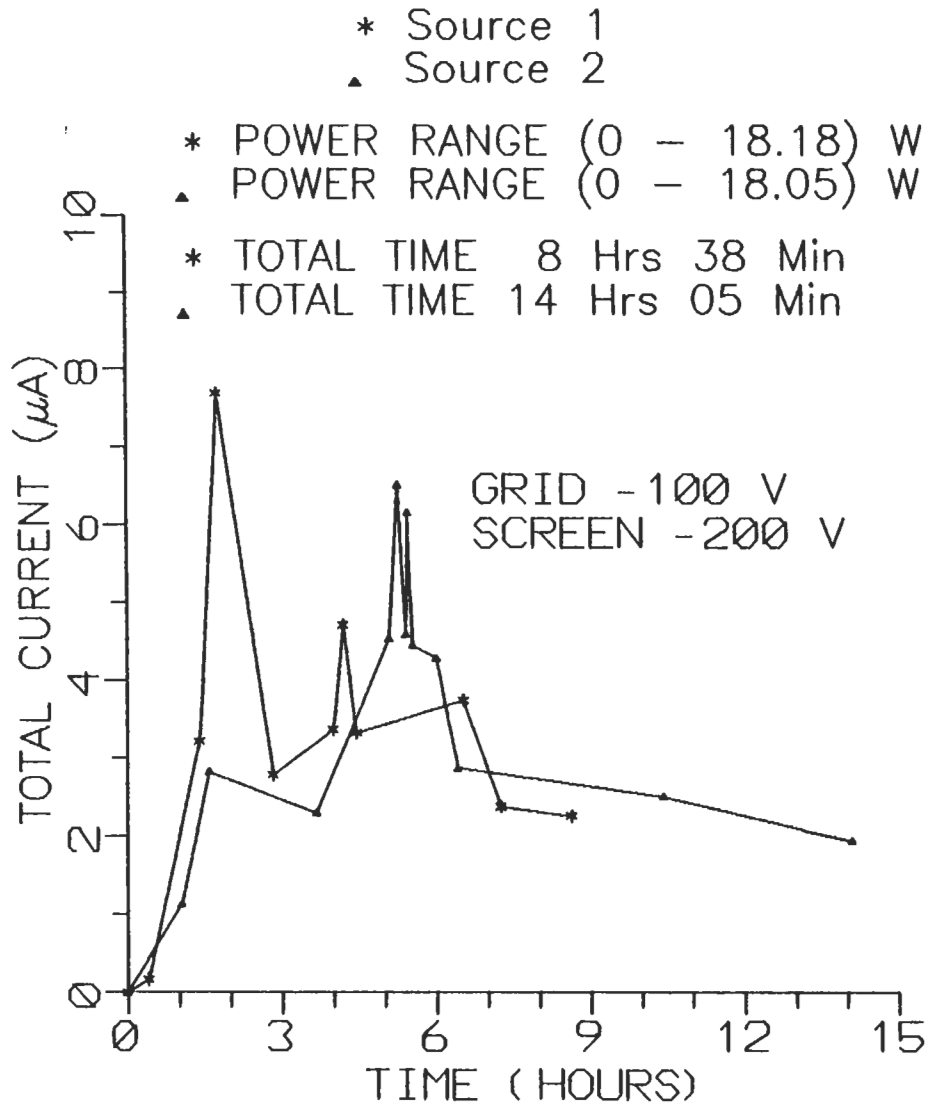


Figure 34. Cesium Lifetimes With Coatings.

CESIUM  
WITH COATING

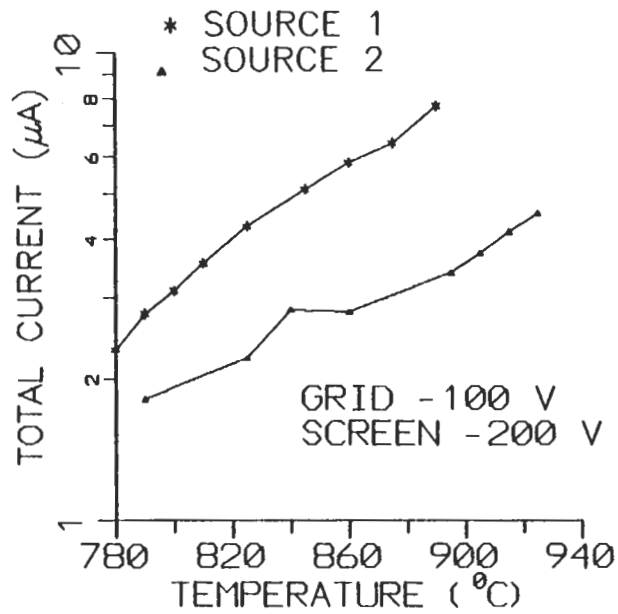
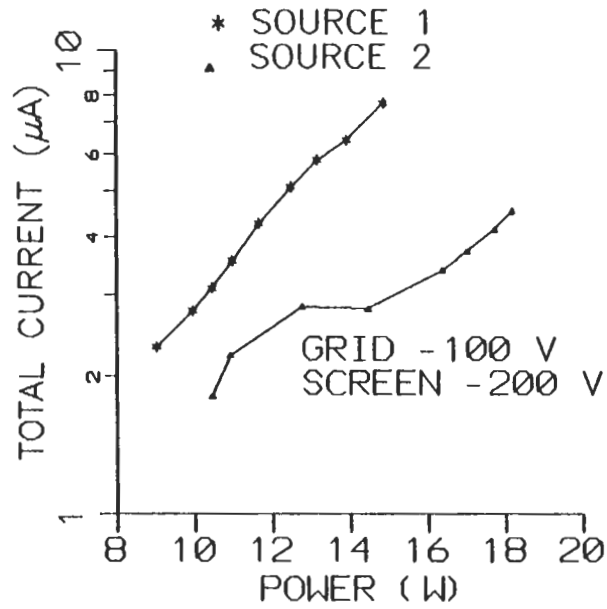


Figure 35. Cesium With Coating Total Currents vs Power and Temperature.

POTASSIUM  
WITH AND WITHOUT  
COATING

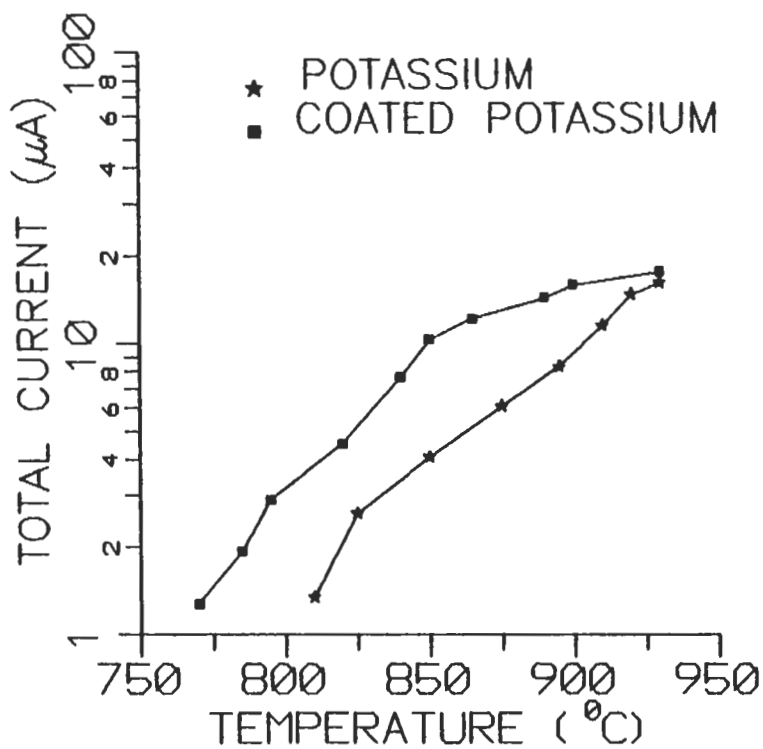


Figure 36. Potassium With and Without Coating Total Current vs Temperature.

CESIUM  
WITH AND WITHOUT  
COATING

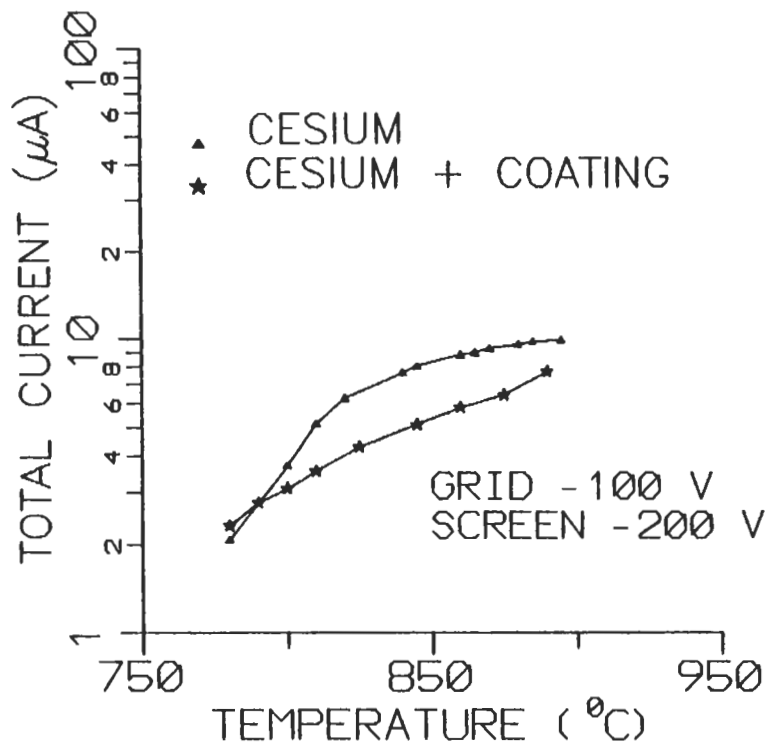


Figure 37. Cesium With and Without Coating Total Current vs Temperature.

# COMPARISON TEMPERATURE °C

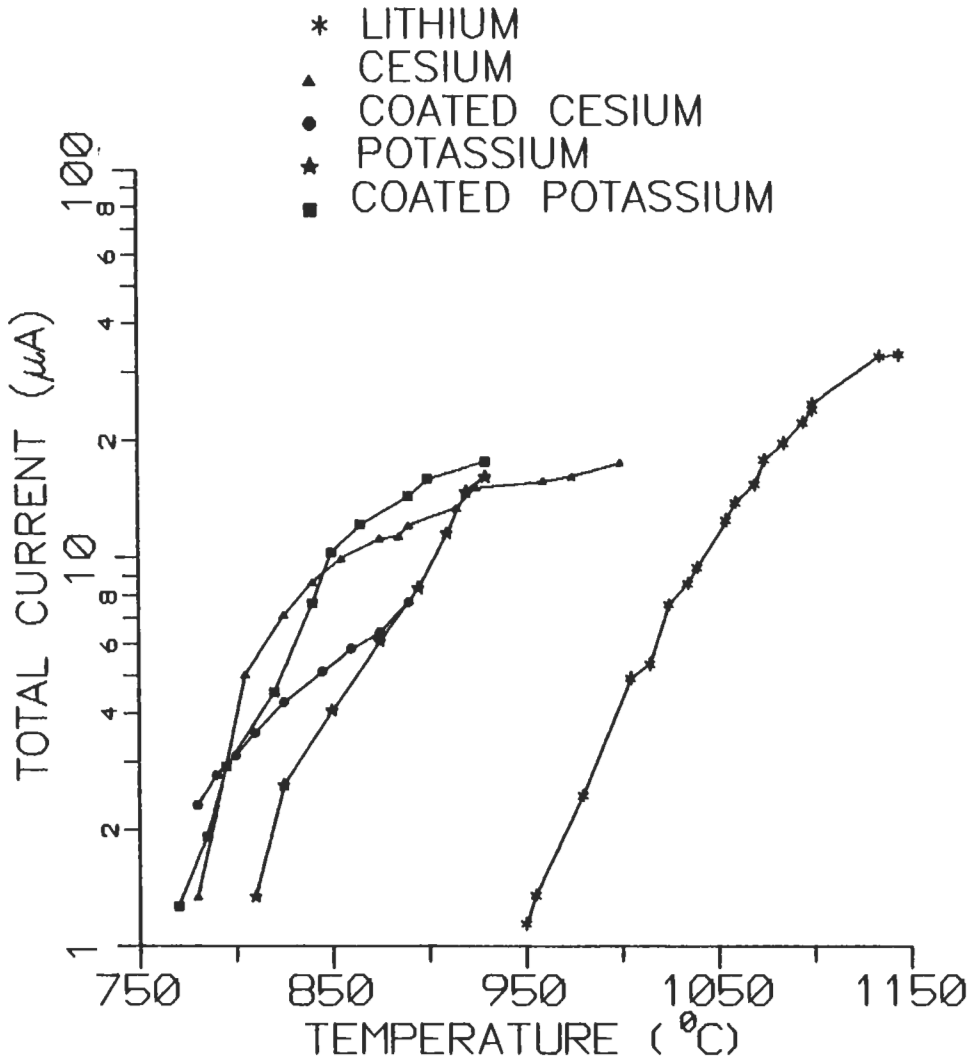
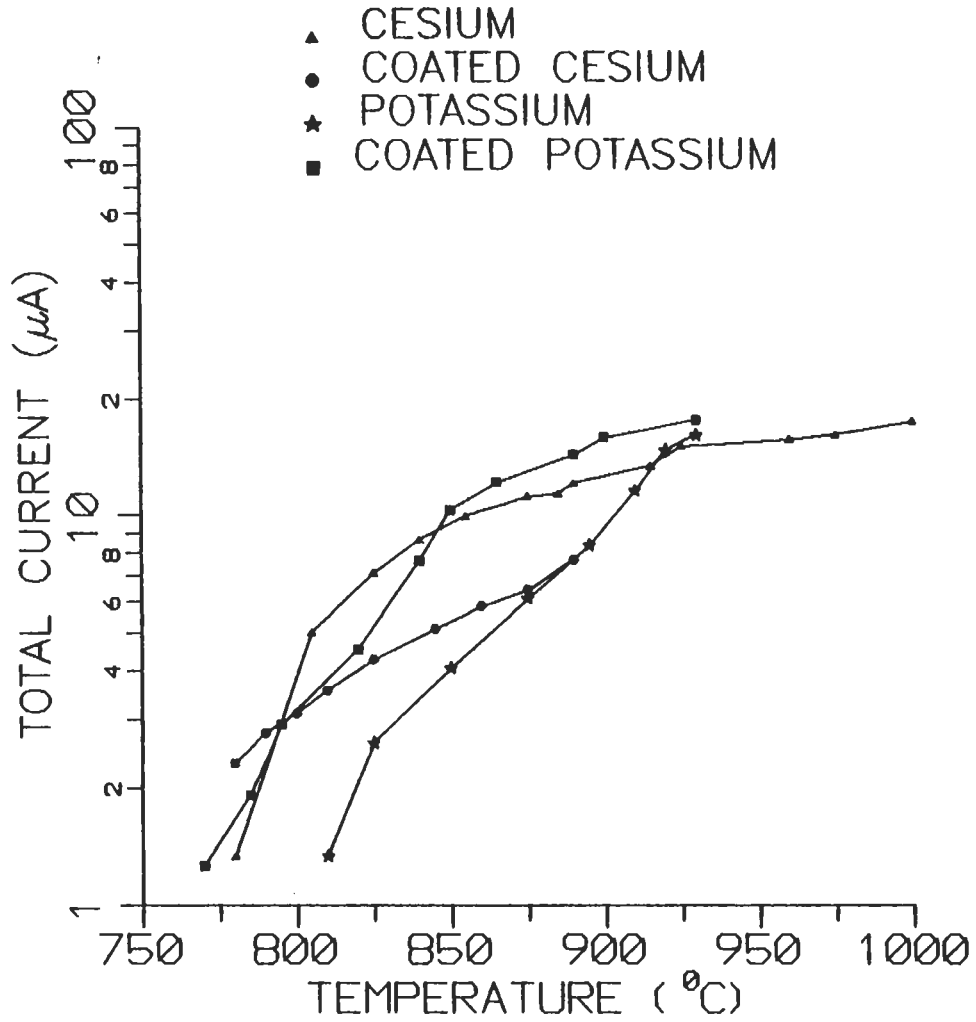


Figure 38. Comparison of all Source Types Total Current vs Temperature.

# COMPARISON TEMPERATURE °C



**Figure 39. Comparison of all Source Types Total Current vs Temperature Below 1000°C.**

## COMPARISON GRID POTENTIAL

*	LITHIUM	1060 °C	27.23 W
▲	CESIUM	925 °C	17.51 W
●	COATED CESIUM	925 °C	18.18 W
★	POTASSIUM	885 °C	14.45 W
■	COATED POTASSIUM	905 °C	16.14 W

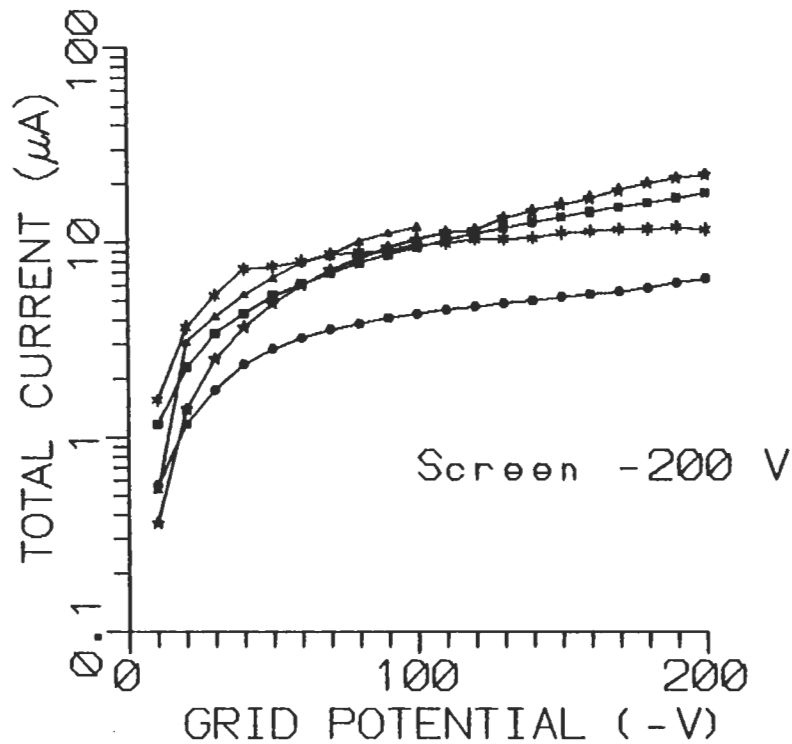


Figure 40. Comparison of all Source Types Total Current vs Grid Potential: All sources were preset to produce 10(μA) current at a Grid Potential of -100(V).

## LIST OF REFERENCES

1. Park, Young-chul, *Hollow Cathode Plasma Source Characteristics*, Master's Theses, Naval Postgraduate School, Monterey, CA, December 1989.
2. Ryu, Chong Soo, *Satellite Charge Control With Lithium Ion Source and Electron Emission*, Master's Theses, Naval Postgraduate School, Monterey, CA, December 1990.
3. Knott, K., Decreau, Korth, A., Pedersen, A., and Wrenn, "The Potential of an Electrostatically Clean Geostationary Satellite and its Use in Plasma," *Journal of Planet and Space Science*, v.32, No.2, pp.227-237, 1984.
4. Tascione, Thomas F., *Introduction to the Space Environment*, pp.97-100, Orbit Book Company, 1988.
5. Olsen, R. C., and Purvis, C. K., "Observations of Charging Dynamics," *Journal of Geophysical Research*, v.88, No.47, pp.5657-5667, 1983.
6. Deforest, S. E., "Spacecraft Charging at Synchronous Orbit," *Journal of Geophysical Research*, v.77, p.651, 1972.
7. Olsen, R. C., "Record Charging Events from Applied Technology Satellite," *Journal of Spacecraft and Rockets*, v.24, No.4, p.362, 1987.
8. Whipple, E. C., "Observation of Photoelectrons and Secondary Electrons Reflected From a Potential Barrier in the Vicinity of ATS-6," *Journal of Geophysical Research*, v.81, No.4, pp.715-719, 1976.
9. Garrett, Henry B., and Pike, Charles P., "Space Systems and Their Interactions with Earth's Space Environment; Spacecraft Charging: A Review (H.B. Garrett)," *Progress in Astronautics and Aeronautics*, v.71, pp.167-226, 1980.
10. Reasoner, D. L., Lennartson, Walter, and Chappell, C. R., "Spacecraft Charging by Magnetospheric Plasmas," *Progress in Astronautics and Aeronautics*, v.47, pp.89-101, 1976.

11. Koons, H. C., Mizera, J. L., Roeder, and Fennell, J. F., "Severe Spacecraft-Charging Event on SCATHA in September 1982," *Journal of Spacecraft and Rockets*, v.25, pp.239-243, 1988.
12. Grard, R., Knott, K., and Pederson, A., "Spacecraft Charging Effects," *Space Science Review*, v.34, p.289, 1983.
13. Gussenhoven, M. S., and Mullen, E. G., "Geosynchronous Environment for Severe Spacecraft Charging," *Journal of Spacecraft and Rockets*, v.20, pp.26-32, 1983.
14. Deininger, W. D., Aston, G., and Pless, L. C., "Hollow Cathode Plasma Source for Active Spacecraft Charge Control," *Review of Scientific Instruments*, v.58(6), p.1053, 1987.
15. ASPOC Scientific/Technical Plan., "Proposal for an Active Spacecraft Potential Control Experiment (ASPOC)-Ion Emitter- for the Stop Cluster Mission," *IWF Oesterreichische Akademie der Wissenschaften*, Inffeldgasse 12, A-8010 Graz. Austria, 1988.
16. Olsen, R. C., "Modification of Spacecraft Potentials by Plasma Emissions," *Journal of Spacecraft and Rockets*, v.18, No.5, pp.462-469, 1981.
17. California Institute of Technology, Pasadena, California, *Quiet Plasma Source*, NASA Tech Brief, by C. J. Morrissey, v.10, No.5, Item 25, 1986.
18. Cobine, James D., *Gaseous Conductors (Theory and Applications)*, pp.123-128, Dover Publishing Inc., 1958.
19. Sampson Milo P., and Bleakney, Walker, "A Mass-Spectrograph Study of Ba, Sr, In, and Na," *Physical Review*, v.50, pp.456-458, 1936.
20. Blewett, J. P., and Jones, E. J., "Filament Sources of Positive Ions," *Physical Review*, v.50, pp.464-468, 1936.
21. Johnson, F. M., "Studies of the Ion Emitter Beta-Eucryptite," *RCA Review*, pp.427-446, 1962.
22. Heinz, Otto, and Reaves, R. T., "Lithium Ion Emitter for Low Energy Beam Experiments," *The Review of Scientific Instruments*, v.39, pp.1229-1230, 1968.

23. Spectra-Mat Inc., Watsonville, California, Ion Emitter Impregnate.
24. Spectra-Mat Inc., Watsonville, California, Technical Bulletin #118, Ion Sources, 1980.

## INITIAL DISTRIBUTION LIST

1. Defense Technical Information Center 2  
Cameron Station  
Alexandria, VA 22304-6145
2. Library, Code 0142 2  
Naval Postgraduate School  
Monterey, CA 93943-5002
3. Department Chairman, Code Ph 1  
Department of Physics  
Naval Postgraduate School  
Monterey, CA 93943-5000
4. Dr. R. C. Olsen, Code Ph/Os 2  
Department of Physics  
Naval Postgraduate School  
Monterey, CA 93943-5000
5. Dr. Otto Heinz, Code Ph/Hz 1  
Department of Physics  
Naval Postgraduate School  
Monterey, CA 93943-5000
6. Mr. Gracen Joiner 1  
Code 1114SP  
Office of Naval Research  
800 N. Quincy Street  
Arlington, VA 22217
7. Dr. Henry Radoski 1  
AFOSR/NP  
Building #410, Bolling AFB  
Washington, DC 20332
8. Mr. Kim Gunther 1  
Spectra-Mat, Inc.  
100 Westgate Drive,  
Watsonville, CA 95076
9. CPT Dean A. Gant 1  
11119 Mallard Crossing Drive,  
Charlotte, NC 28262

10. Dr. E. C. Whipple 1  
NASA/HQ/SS-1  
Washington, DC 20546
11. Major C. W. Beatty 1  
DNA/RAEV  
6801 Telegraph Road  
Alexandria, VA 22310-3398
12. Mr. Herb Cohen 1  
W. J. Schafer Assoc. Inc.  
1901 N. Fort Meyer Drive  
Suite 800  
Arlington, VA 22209



